

Review

Open Access



Fundamentals and perspectives of electrolyte additives for non-aqueous Na-ion batteries

Vadim Shipitsyn^{1,2,*} , Nicholas Antrasian^{3,#}, Vijayendra Soni³, Linqin Mu^{3,*} , Lin Ma^{1,2,*} 

¹Department of Mechanical Engineering and Engineering Science, The University of North Carolina at Charlotte, Charlotte, NC 28223, USA.

²Battery Complexity, Autonomous Vehicle and Electrification (BATT CAVE) Research Center, The University of North Carolina at Charlotte, Charlotte, NC 28223, USA.

³School of Engineering for Matter, Transport, and Energy, Arizona State University, Tempe, AZ 85281, USA.

#These authors contributed equally.

* **Correspondence to:** Prof. Linqin Mu, School of Engineering for Matter, Transport, and Energy, Arizona State University, 336E Orange St, Tempe, AZ 85281, USA. E-mail: linqinmu@asu.edu; Prof. Lin Ma, Department of Mechanical Engineering and Engineering Science, The University of North Carolina at Charlotte, 9201 University City Blvd, Charlotte, NC 28223, USA. E-mail: l.ma@charlotte.edu

How to cite this article: Shipitsyn V, Antrasian N, Soni V, Mu L, Ma L. Fundamentals and perspectives of electrolyte additives for non-aqueous Na-ion batteries. *Energy Mater* 2023;3:300038. <https://dx.doi.org/10.20517/energymater.2023.22>

Received: 4 Apr 2023 **First Decision:** 28 Apr 2023 **Revised:** 11 Jun 2023 **Accepted:** 25 Jun 2023 **Published:** 1 Sep 2023

Academic Editors: Elie Paillard, Yuping Wu **Copy Editor:** Pei-Yun Wang **Production Editor:** Pei-Yun Wang

Abstract

Despite extensive research efforts to develop non-aqueous sodium-ion batteries (SIBs) as alternatives to lithium-based energy storage battery systems, their performance is still hindered by electrode-electrolyte side reactions. As a feasible strategy, the engineering of electrolyte additives has been regarded as one of the effective ways to address these critical problems. In this review, we provide a comprehensive overview of recent progress in electrolyte additives for non-aqueous SIBs. We classify the additives based on their effects on specific electrode materials and discuss the functions and mechanisms of each additive category. Finally, we propose future directions for electrolyte additive research, including studies on additives for improving cell performance under extreme conditions, optimizing electrolyte additive combinations, understanding the effect of additives on cathode-anode interactions, and understanding the characteristics of electrolyte additives.

Keywords: Non-aqueous Na-ion batteries, electrolyte additives, solid electrolyte interphase, cathode electrolyte interphase, cell lifetime



© The Author(s) 2023. **Open Access** This article is licensed under a Creative Commons Attribution 4.0 International License (<https://creativecommons.org/licenses/by/4.0/>), which permits unrestricted use, sharing, adaptation, distribution and reproduction in any medium or format, for any purpose, even commercially, as long as you give appropriate credit to the original author(s) and the source, provide a link to the Creative Commons license, and indicate if changes were made.



INTRODUCTION

Regulating atmospheric concentrations of greenhouse gas is a critical step toward curbing the potentially catastrophic consequences of climate change, including unprecedented wildfires, extreme weather, and acidification of the oceans. One of the key priorities in this effort is the transition from fossil fuels to renewable energy sources. As an electrochemical energy storage technology, the lithium-ion battery (LIB) has been predominantly deployed among grid-scale energy storage and electric vehicles (EVs) to support such a carbon-neutral energy transition by storing intermittent renewable energy sources with reliable durability, compelling energy density, and declining costs. However, rapidly growing demands in many other energy sectors (e.g., energy grid storage systems and electric bicycles) require reliable, affordable, and complementary electrochemical energy storage systems to circumvent the key resource crisis of lithium. The sodium-ion battery (SIB) has been regarded as one of the promising routes to complement LIB technology by its integration into those applications that do not demand requirements on the cell energy density (e.g., grid energy storage system). This is ascribed to the abundant availability of sodium (Na) and the discovery of electrode materials with cheap and abundant elements, such as carbon, copper, manganese, and iron^[1-4].

Despite the surging research interest and achievements in the development of SIBs over the past few years, the insufficient lifetime of SIBs, especially under harsh operation conditions, greatly impedes their large-scale deployment. Similar to a LIB, a typical SIB is composed of a cathode, anode, electrolyte (with sodium salts dissolved in non-aqueous solvents), separator, and current collector (Al-foil for both cathode and anode materials). To extend the cell lifetime and improve cell safety, significant efforts have been made by fabricating artificial interphase, performing pre-sodiation, and regulating electrolyte components, especially electrolyte additives, because additives enable efficient modifications on the interphases where side reactions occur between electrodes and electrolytes. To realize the importance of electrolyte additive studies, more detailed discussions on the interphase will be illustrated in the next section.

Currently, there are many comprehensive reviews in the field of SIBs covering various aspects, including a general overview of SIBs^[1,4,5], the development and prospects of cathode materials^[6-8], research progress of non-aqueous liquid electrolytes and relevant interphases^[9-11], the progress and strategies for stabilizing anode in SIBs^[12-14], *etc.* However, there have been few prospective reviews of electrolyte additives in non-aqueous SIBs. Considering that the use of electrolyte additives is closely related to the performance of the cathode, anode, and electrolyte, a timely review with an academic perspective in this area is urgently needed. Such a review would summarize our current understanding of Na-ion-containing liquid electrolytes and provide significant assistance for the further development of SIBs. Herein, a systematic and comprehensive summary of the functions of electrolyte additives used in non-aqueous SIBs was introduced in this work. We particularly highlighted the fundamental scientific understanding of the effects of different electrolyte additives on different anode and cathode materials, respectively. Moreover, the outlook on the development of Na-ion electrolyte additives regarding tolerance on extreme conditions (i.e., fast charging, wide temperature range), development of electrolyte additive combinations, understanding the effect of additives on cathode-anode interaction, understanding the characteristics of electrolyte additives, and designing of novel electrolyte additives for improving cell safety was proposed.

INTERPHASE FORMATION MECHANISMS AND CHARACTERIZATIONS

In principle, electrode materials should be operated within the electrochemical stability window of a certain electrolyte system. The operating voltage of an electrolyte is determined by the highest occupied molecular orbital (HOMO) and the lowest unoccupied molecular orbital (LUMO). However, the Fermi energy of many electrode materials surpasses the HOMO or LUMO of the electrolyte^[15], which leads to the electrolyte

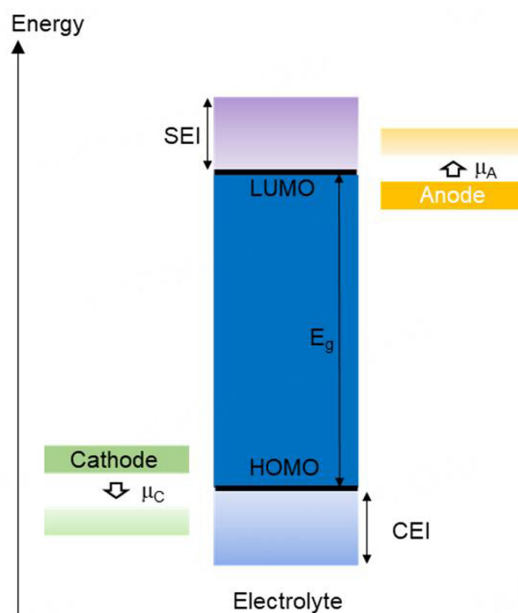


Figure 1. A schematic of the SEI/CEI formation under electrochemical reduction/oxidation conditions. CEI: Cathode electrolyte interphase; HOMO: highest occupied molecular orbital; LUMO: lowest unoccupied molecular orbital; SEI: solid electrolyte interphase.

reduction or oxidation upon discharging or charging, resulting in by-products at the electrode surface, i.e., solid electrolyte interphase (SEI) on the anode and the cathode electrolyte interphase (CEI) on the cathode, respectively. The electrode-electrolyte interphase (EEI) is usually working ion (e.g., Li^+ , Na^+) conductive but electrically insulating, leading to a physical barrier for the continuing side reactions. This is the reason why many electrode materials outside the LUMO or HOMO can still be operated with a reasonable cycle life [Figure 1]. Because of that, the chemical and structural characteristics of an EEI layer are crucial to the overall battery performance. Thus, significant efforts have been conducted, including attempts to decipher the formation mechanisms, composition, and microstructure of the EEI that originate from the interactions between the active materials and electrolytes. It has been confirmed that CEI/SEI consists of a multi-layered structure, i.e., an inorganic inner layer and an organic outer layer^[10]. The inorganic species, including Na_2CO_3 and NaF , allow Na^+ to diffuse and block electrons, while the organic species of RONA and sodium ethylene decarbonate (Na_2EDC) are highly dependent on the solvent for transporting Na^+ . CEI/SEI in SIBs is generally non-uniform, porous, heterogeneous, and fragile, with thicknesses ranging from a few to tens of nanometers. Thus, constructing a robust EEI layer becomes one of the research streams to enable long-duration batteries.

Typically, all the electrolyte components, including solvents, salts, and electrolyte additives, could decompose and form EEIs on both the cathode and anode. It is obvious that the use of electrolyte additives is one of the most viable, economical, and efficient approaches to form an EEI and improve cell performance due to their small amount (a threshold of 10% is adopted here, as indicated by Xu^[16]). As a result of the decomposition of additives, a layer of their chemical signatures will be formed with a function of conducting Na^+ cations and blocking electron transfer. In this review, we will focus on the interfacial chemistry between different electrodes and electrolytes and summarize the roles of various additives in influencing cell behavior. The review will cover current understandings of the composition and structure of the EEIs in SIBs and the effects of various functional electrolyte additives on such EEIs.

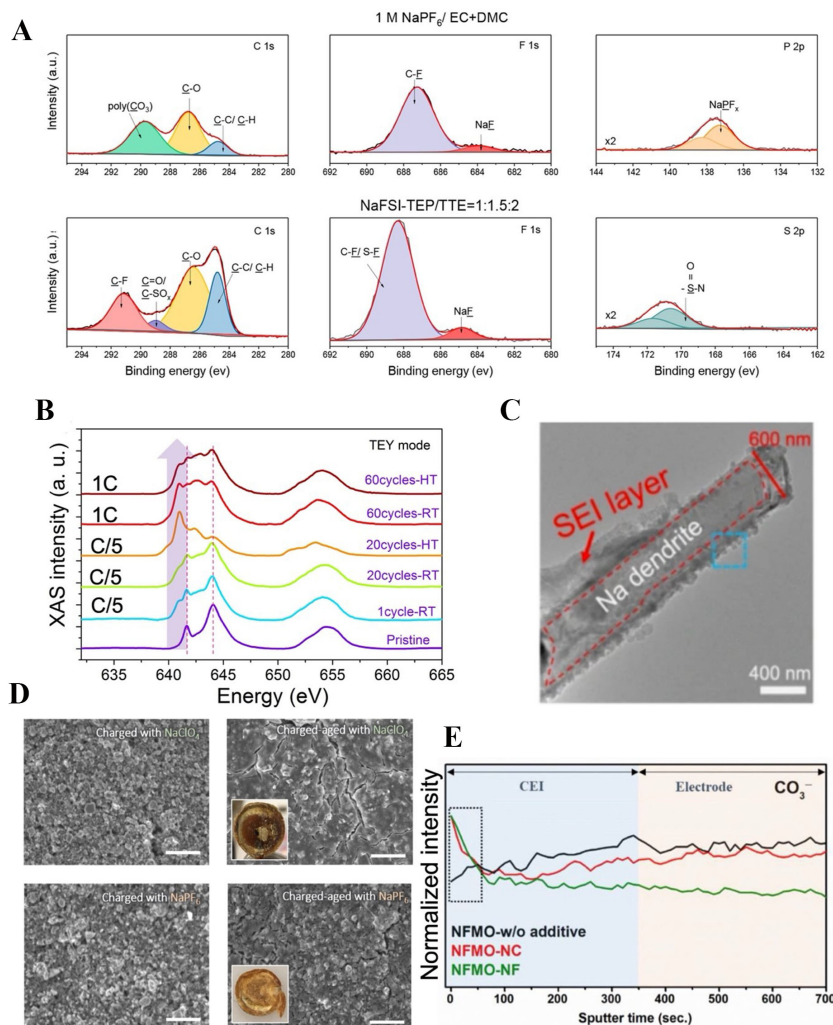


Figure 2. Exemplar characterizations used for the EEI studies. (A) XPS characterization for C 1s, F 1s, and S 2p spectra of the CEI components on the $\text{NaCu}_{1/9}\text{Ni}_{2/9}\text{Fe}_{1/3}\text{Mn}_{1/3}\text{O}_2$ (Na-CNFM) cathode after the 10th cycle in the electrolytes of 1 M $\text{NaPF}_6/\text{EC}+\text{DMC}$ and NaFSI-triethyl phosphate (TEP)/1,1,2,2-tetrafluoroethyl-2,2,3,3-tetrafluoropropyl ether (TTE) Reproduced from ref^[17]; copyright 2020 American Chemical Society; (B) Soft XAS Mn L-edge spectra in the TEY mode for the $\text{NaNi}_{1/3}\text{Fe}_{1/3}\text{Mn}_{1/3}\text{O}_2$ cathode after different cycling histories. Reproduced from ref^[18]; copyright 2018 Wiley; (C) Cryo-TEM of the Na dendrite at low magnification in FEC-free EC:DMC-based electrolyte at the first cycle. Reproduced from ref^[19]; copyright 2021 Springer Nature; (D) SEM images of charged NaFeO_2 electrodes before and after an aging cycling step (inset image: glass fiber separator after aging). Reproduced from ref^[20]; copyright 2022 IOP Publishing Limited; (E) TOF-SIMS depth profiles of inorganic secondary ion fragments on the surfaces of the one-cycle $\text{Na}_{0.67}\text{Fe}_{0.5}\text{Mn}_{0.5}\text{O}_2$ electrodes showing the evolution of CO_3^- species in the CEI layer formed on the electrode surface. Reproduced from ref^[21]; copyright 2021 Elsevier. CEI: Cathode electrolyte interphase; DMC: dimethyl carbonate; EC: ethylene carbonate; EEI: electrode-electrolyte interphase; FEC: fluoroethylene carbonate; SEI: solid electrolyte interphase; SEM: scanning electron microscopy; TEM: transmission electron microscopy; TEY: total electron yield; TOF-SIMS: time-of-flight secondary ion mass spectrometry; XAS: X-ray absorption spectroscopy; XPS: X-ray photoelectron spectroscopy.

We first need to understand the chemical and physical properties of EEI layers to inform the formulation of additives. However, it is challenging to qualify EEIs experimentally due to the characteristics of nano-scale inhomogeneous layers; thus, the currently employed characterizations are heavily based on surface-sensitive techniques. Herein, we summarize several representative techniques that are generally utilized in the SIB system [Figure 2]^[17-21]. X-ray photoelectron spectroscopy (XPS, Figure 2A) is the commonly used tool that can compositionally reveal EEIs since it provides depth-dependent information on the chemical bonding characteristics within the depth of 10 nm^[22-24]. For a deeper characterization down to ~100 nm, soft X-ray

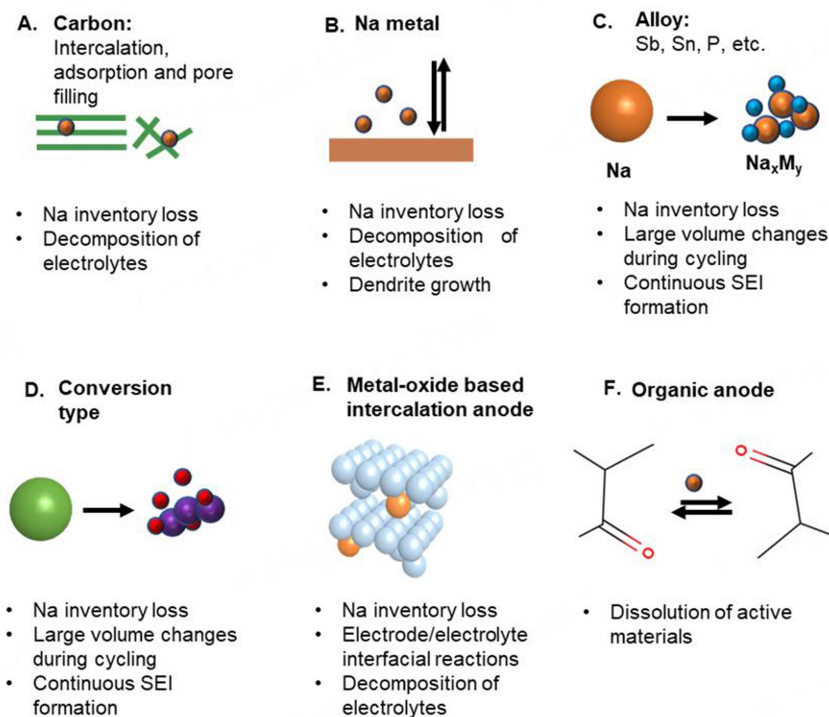


Figure 3. A schematic of Na storage mechanisms of different types of anode materials.

absorption spectroscopy (XAS, [Figure 2B](#)) can provide the electronic structure of the cathode surface by probing the oxygen K-edge and transition metal (TM) L-edge^[25-27]. By virtue of ensemble-averaged soft XAS, we can differentiate the oxidation state and local environment of the central element in the top surface (~5 nm), sub-surface (~10 nm), and the bulk (~50 nm) by applying Auger Electron Yield (AEY), Total Electron Yield (TEY), and Fluorescence Yield (FY) modes. It provides a comprehensive understanding of the structural and chemical rearrangement on the cathode surface. In addition, transmission electron microscopy (TEM) can be used to visualize the atomic structure in bulk and at the edge of a single particle. However, relying solely on TEM images to represent the general behavior of all active materials may be insufficient due to the small observing area (~nm). Thus, it is necessary to employ additional tools, e.g., soft XAS and XPS, to supplement TEM observations. For SEI studies on sodium metal, we need to incorporate Cryo-TEM [[Figure 2C](#)] and lower radiation dose to protect the beam-sensitive SEI layers^[19,28,29]. Regarding morphology, scanning electron microscopy (SEM, [Figure 2D](#)) is a widely used technique that can provide a rough surface morphology but may lose the fine resolution. X-ray diffraction (XRD) is used to identify crystalline structures with a probing depth on the order of micrometers, while energy-dispersive X-ray spectroscopy (EDX) allows for the chemical characterization of substances^[30,31]. Other techniques, including electrochemical impedance spectroscopy (EIS^[32]), time-of-flight secondary ion mass spectrometry (TOF-SIMS^[33], [Figure 2E](#)), and inductively coupled plasma atomic emission spectroscopy (ICP-AES^[34]), can give useful information on EEI impedance, interphase composition, and chemical identity and concentration. Detailed examples on understanding the effect of additives on EEI with these techniques will be discussed in the next two sections.

ELECTROLYTE ADDITIVES FOR IMPROVING ANODE PERFORMANCE

Most commonly used anode materials have different Na storage mechanisms, resulting in different challenges to achieving high reversibility [[Figure 3](#)]. Anode additives are expected to overcome these

challenges by regulating SEI formation due to their higher reduction potentials compared to electrolyte solvents and salts. Thus, we will discuss the additives according to different anode materials in the following sections.

Carbonaceous anode

Carbonaceous materials, including both “soft carbon” and “hard carbon” (HC), are the most dominant candidates for commercial metal ion batteries (MIBs) due to their high specific capacity, relative ease of production, and low cost. Unlike LIBs, attempts to use graphite as an anode material in SIBs were not successful, with a trivial reversible capacity of $\sim 12 \text{ mAh g}^{-1}$ during the first cycles^[35]. Instead of graphite, non-graphitizing carbon material with a disordered structure (so-called “HC”) is used in sodium systems, which will be the focus of this work.

The electrochemical performance of HC is highly sensitive to its annealing temperature during synthesis, which was proven by many studies^[36,37]. However, only the influence of electrolyte composition on electrochemical characteristics will be discussed in this review. The issue of a high irreversible capacity is very typical for HC material and can be attributed to the SEI formation due to the low intercalation voltage around $\sim 0 \text{ V vs. Na}^+/\text{Na}$. A robust SEI is very crucial for extending the lifetime of a cell, so it is important to realize what additives and how they affect the SEI formation. As an overview, [Tables 1](#) and [2](#) summarize the effect of selected electrolyte additives on the irreversible capacity and capacity retention of HC/Na half-cells and HC-based full-cells, respectively. Detailed functional mechanisms classified by additive chemistries will be discussed in the following sections.

Fluorine-containing additives

Certain fluorine-containing compounds have a lower LUMO compared to carbonate solvents, which makes them suitable candidates to modify the SEI and improve the anode reversibility. Fluoroethylene carbonate (FEC, [Table 3](#)) is the most effective additive for the formation of reliable SEI. There was a conclusion in some papers that the addition of FEC (2%-3% *vol.*) as an additive decreases initial Coulombic efficiency (ICE, [Table 1](#)) and increases the overpotential between charge and discharge^[46,71]. However, in an earlier report by Komaba *et al.*^[39], it was discussed that the FEC addition does not affect the capacity and Coulombic Efficiency (CE) at the first cycle and improves electrochemical performance in all cases. Komaba *et al.* noticed that the addition of 10% *vol.* of FEC impairs cell performance, from which it was concluded that an addition of 2% of FEC was the most acceptable amount. A similar conclusion was made by Kim *et al.*^[63], who stated that 0.5 *wt.*% FEC in electrolytes hardly improves the cyclability of HC symmetric cells. However, they found that it has a positive effect on HC/Na cells.

To understand the working principle of FEC additives, XPS was employed to reveal the chemical information of the surface of HC after cycling. Species are present with Na_2CO_3 [binding energy (BE) $\approx 290 \text{ eV}$ for CO_3], R-COONa (BE $\approx 286.6 \text{ eV}$ for CO), and NaF (BE $\approx 687 \text{ eV}$) [[Figure 4A-C](#)]. In addition, the peak, representing NaF species, increases with a higher FEC concentration, which validates the statement that FEC enhances the formation of the inorganic compound NaF. The same contribution of FEC in the SEI formation was noticed in the electrolyte sodium bis(trifluoromethanesulfonyl)imide (NaTFSI) + EC:DMC (1:1). In many studies, NaF is assumed as an efficient passivation agent, which forms through the decomposition of FEC^[72]. Here, the reaction process on the surface of HC is provided below^[73]:



Table 1. A summary of the electrochemical performance of the carbonaceous anode with metallic sodium as the counter electrode

Material	Salt	Solvent	Additive	ICE, %	C _v , mAh/g	C _{n^r} , mAh/g	N	Ref.		
HC	1M NaClO ₄	EC	-	88.0	227	212	80	Komaba et al., 2011 ^[38]		
		PC	-	79.0	238	225	90			
			-	89.7	226	100	50	Komaba et al., 2011 ^[39]		
HCNS				85.1	245	20	100	Dahbi et al., 2016 ^[40]		
HC			2% vol. VC	41.5	223	165	100	Tang et al., 2012 ^[41]		
				72.0	100	-	-	Komaba et al., 2011 ^[38]		
HC			2% vol. FEC	73.7	101	70	50	Komaba et al., 2011 ^[39]		
			10% vol. FEC	90.1	220	175	100			
			0.2% vol. DFEC	86.1	240	110	100	Dahbi et al., 2016 ^[40]		
			2% vol. DFEC	89.4	202	149	40	Komaba et al., 2011 ^[39]		
			2% vol. DFEC	84.0	137	139	10			
CNF		EC/PC (1:1)	-	68.0	76	55	35			
HDC				58.8	262.9	176	600	Luo et al., 2013 ^[42]		
HHC				57.6	246	225	180	Zhou and Guo, 2014 ^[43]		
HC				65.9	274	261	150	Xie et al., 2020 ^[44]		
				89.3	180	125	500	Bommier et al., 2014 ^[45]		
HC				61.0	325	190	30	Ponrouch et al., 2013 ^[46]		
				-	310	175	30			
				EC/DMC (1:1)	-	49.0	210	110	30	Komaba et al., 2011 ^[38]
					63.0	310	274	100	Zhu et al., 2017 ^[47]	
					63.0	261	206	700		
					70.5	274	247	200	Jin et al., 2014 ^[48]	
					5% vol. FEC	64.4	80	60	2,000	Yang et al., 2016 ^[49]
					2% vol. FEC	82.5	226	179	65	Komaba et al., 2011 ^[39]
				PC/DMC(1:1)	-	82.0	238	0	10	
				EC/EMC (1:1)	-	76.5	225	170	45	Komaba et al., 2011 ^[38]
HCNW				50.5	251	206.3	400	Cao et al., 2012 ^[50]		
HC		EC/DEC (1:1)		78.0	240	225	100	Komaba et al., 2011 ^[38]		
				67.8	339	298	300	Lotfabad et al., 2014 ^[51]		
				67.8	350	210	600			
				74.1	264	245	35	Jiang et al., 2018 ^[52]		
				83.0	312	290	100	Li et al., 2014 ^[53]		
				53.5	280	266	100	Li et al., 2013 ^[54]		
				57.5	298	255	200	Ding et al., 2013 ^[55]		
HC		BC	-	84.0	236	90	50	Komaba et al., 2011 ^[38]		
HC	0.91M NaClO ₄	TMP	-	-	negligible	-	-	Liu et al., 2018 ^[56]		
			5% vol. FEC	47.6	114.4	-	-			
			-	45.6	232.3	-	-			
			5% vol. FEC	62.5	210.9	-	-			
			-	67.1	256.1	170	50			
HC	2.50M NaClO ₄		5% vol. FEC	68.4	243.8	70	1,500			
			86.7	242	95	100	Dahbi et al., 2016 ^[40]			
			0.5% vol. FEC	88.1	250	220				
HC	1M NaPF ₆	PC	-	88.0	247	219				
			1% vol. FEC	86.0	240	180				
			2% vol. FEC	86.0	240	180				
			EC/PC (1:1)	-	89.7	255	130			
			0.5% vol. FEC	87.9	248	215				

			2% vol. FEC	87.5	238	170		
		EC/DMC (1:1)	-	83.0	315	305	100	Li <i>et al.</i> , 2016 ^[57]
				81.0	358	312	200	Li <i>et al.</i> , 2019 ^[58]
			1.5% vol. FEC	72.0	220	158	130	Fondard <i>et al.</i> , 2020 ^[24]
			3% vol. FEC	77.0	230	216	130	
			1.5% vol. DMCF	48.0	150	120	130	
			3% vol. DMCF	27.0	100	70	130	
			-	80.2	-	-	-	Zhang <i>et al.</i> , 2022 ^[59]
			1% wt. 1,3-PS	81.8				
			1% wt. DTD	86.6				
NCCF		EC/DMC (3:7)	-	-	160	144	1,600	Shao <i>et al.</i> 2013 ^[60]
AC		EC/DEC (1:1)	-	22.2	80	63	200	Feng <i>et al.</i> , 2015 ^[61]
			5% vol. EFPN	27.6	94	92	200	
HC			-	83.0	235	213	300	Luo <i>et al.</i> , 2015 ^[62]
			-	88.0	255	65	100	Kim <i>et al.</i> , 2019 ^[63]
			0.5 wt.% FEC	84.0	248	95		
			0.5 wt.% SA	80.0	251	150		
		DME	-	84.7	235	170	2,000	Bai <i>et al.</i> , 2019 ^[64]
			0.5% vol. VC	83.0	221	211	2,000	
			1% vol. VC	74.3	-	-	-	
			5% vol. VC	41.7	-	-	-	
			10% vol. VC	30.1	-	-	-	
		VC	-	21.3	-	-	-	
HC	0.8 M NaPF ₆	EC/PC (1:4)	2% vol. FEC	76.2	274	221	100	Che <i>et al.</i> , 2017 ^[65]
			2% vol. FEC + 0.05M RbPF ₆	78.9	297	283		
			2% vol. FEC + 0.05M CsPF ₆	78.5	302	293		
HC	0.9M NaFSI	TFEP	-	75.4	239	219	100	Jiang <i>et al.</i> , 2018 ^[52]
HC	1.0M NaFSI	TMP	-	<1.0	no discharge capacity	-	-	Wang <i>et al.</i> , 2017 ^[66]
			2.0M NaFSI	48.0	-	-	-	
			3.3M NaFSI	75.0	238	225	1,200	
HC	1M NaTFSI	EC/DMC (1:1)	-	65.0	190	80	130	Fondard <i>et al.</i> , 2020 ^[24]
			3% vol. FEC	68.0	205	185	110	
			3% vol. DMCF	60.0	208	150	130	
rGO	1M NaOTf	EC/DEC (1:1)	-	39.0	375	262	100	Zhang <i>et al.</i> , 2016 ^[67]
		DGM	-	74.6	562	509	100	
			-	74.6	332	250	1,000	

The electrochemical performance (CE at the 1st cycle, capacity at the 1st and further cycles) of carbonaceous anodes in various electrolytes is provided. The most frequently used salts are NaPF₆, NaClO₄, and NaFSI. AC: Acetylene black; CNF: carbon nano-fibers; CNSF: carbon nanosheet frameworks; DEC: diethyl carbonate; DFEC: difluoroethylene carbonate; DGM: diglyme; DMC: dimethyl carbonate; DMCF: fluorinated dimethyl carbonate; DME: dimethoxyethane; DTD: 1,3,2-dioxathiolane-2,2-dioxide; EC: ethylene carbonate; EFPN: ethoxy(pentafluoro)cyclotriphosphazene; EMC: ethyl methyl carbonate; FEC: fluoroethylene carbonate; HC: hard carbon; HCN: hollow carbon nanospheres; HCNW: hollow carbon nanowires; HDC: highly disordered carbon; HHC: hydrophilic hard carbon; NaFSI: sodium bis-(fluorosulfonyl)imide; NaTFSI: sodium bis(trifluoromethanesulfonyl)imide; NCCF: nanocellular carbon foam; PC: propylene carbonate; rGO: reduced graphene oxide; SA: succinic anhydride; TFEP: tri(2,2,2-trifluoroethyl) phosphite; TMP: trimethyl phosphate; VC: vinylene carbonate.

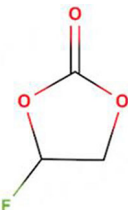
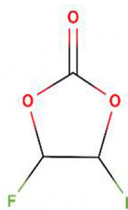
Difluoroethylene carbonate (DFEC, Table 3) was considered as a possible additive for the HC anode, and it is widely used for improving the characteristics of LIBs^[74,75]. However, Komaba *et al.*^[39] concluded that this

Table 2. A summary of the electrochemical performance of full cells with HC anodes in different electrolytes to avoid the effect of an excess Na resource from the metallic sodium anode

Cathode	Electrolyte	Additive	CE at the 1st cycle, %	Discharge capacity at the 1st cycle, mAh/g	Discharge capacity at the <i>n</i> th cycle, mAh/g	Number <i>n</i> of cycles	Ref.
Na _{2/3} Ni _{1/3} Mn _{2/3} O ₂	1M NaClO ₄ + EC/DEC (1:1)	-	76	300	228	150	Li <i>et al.</i> , 2014 ^[53]
NaNi _{1/2} Mn _{1/2} O ₂	1M NaClO ₄ + PC	-	-	215	75	100	Komaba <i>et al.</i> , 2011 ^[38]
	1M NaPF ₆ + PC	-	-	247	118	100	
	1M NaTFSa + PC	-	-	249	105	100	
Na ₃ V ₂ (PO ₄) ₂ F ₃	1M NaPF ₆ + EC/DMC (1:1)	-	83.0	109	71	60	Cometto <i>et al.</i> , 2019 ^[68]
		1% TMSPI	76.0	110	93	60	
		3% VC	88.0	108	95	60	
		0.5% NaODFB	85.0	107	31	60	
		0.5% NaODFB + 1% TMSPI	70.0	109	95	60	
0.5% NaODFB + 1% TMSPI + 3% VC	83.0	110	109	60			
Na ₃ V ₂ (PO ₄) ₂ F ₃	1M NaPF ₆ + EC/PC (1:1)	-	-	-	-	-	Yan <i>et al.</i> , 2019 ^[69]
NaNi _{1/3} Fe _{1/3} Mn _{1/3} O ₂	1M NaPF ₆ + PC/EMC (1:1)	2% FEC	-	950 mAh	726 mAh	750	Che <i>et al.</i> , 2018 ^[70]
		2% FEC + 1% PST	-	950 mAh	802 mAh	1,000	
		2% FEC + 1% PST + 1% DTD	-	950 mAh	876 mAh	1,000	
Na ₃ V ₂ (PO ₄) ₃	0.9M NaFSI + TFEP	-	70.6	87	72	10,000	Jiang <i>et al.</i> , 2018 ^[52]
Na[Cu _{1/9} Ni _{2/9} Fe _{1/3} Mn _{1/3}]O ₂	1M NaClO ₄ + EC/DMC/PC (1:1:1)	2% FEC	74.0	252	175	2,000	Li <i>et al.</i> , 2019 ^[58]
Na(Ni _{0.4} Mn _{0.4} Cu _{0.1} Ti _{0.1}) _{0.999} La _{0.001} O ₂	1M NaPF ₆ + EC/DMC (1:1)	2% wt. FEC	72.3	144.3	84.7	50	Zhang <i>et al.</i> , 2022 ^[59]
		2% wt. FEC + 2% wt. 1,3-PS	76.7	152.6	125.1		
		2% wt. FEC + 2% wt. DTD	79.1	152.4	121.0		
		2% wt. FEC + 0.2% wt. PES	65.3	139.2	36.3		

DEC: Diethyl carbonate; DMC: dimethyl carbonate; DTD: 1,3,2-dioxathiolane-2,2-dioxide; EC: ethylene carbonate; FEC: fluoroethylene carbonate; HC: hard carbon; NaFSI: sodium bis-(fluorosulfonyl)imide; NaODFB: sodium (oxalate) difluoro borate; PC: propylene carbonate; PES: prop-1-ene-1,3-sultone; PS: 1,3-propane sultone; PST: prop-1-ene-1,3-sultone; TFEP: tri(2,2,2-trifluoroethyl) phosphite; TMSPI: tris(trimethylsilyl) phosphite; VC: vinyl carbonate; 1,3-PS: 1,3-propylene sulfite.

Table 3. Fluorine-containing additives

Chemical name of the additive	Fluoroethylene carbonate (FEC)	Difluoroethylene carbonate (DFEC)
Chemical structure of additive		

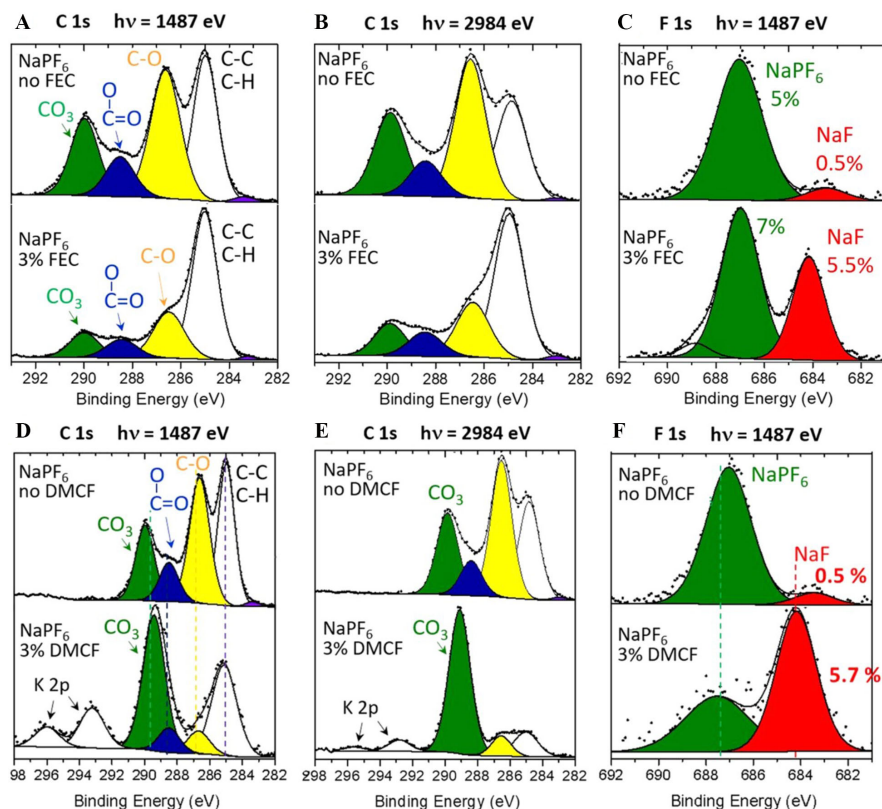


Figure 4. XPS spectra of HC electrodes after 135 cycles in half-cells with NaPF₆/EC:DMC electrolyte. The effect of 3% FEC: (A), (B) C1s and (C) F1s; the effect of 3% DMCF: (D), (E) C1s and (F) F1s. Reproduced from ref^[24], copyright 2020 IOP Publishing Limited. DMC: Dimethyl carbonate; DMCF: fluorinated dimethyl carbonate; EC: ethylene carbonate; FEC: fluoroethylene carbonate; HC: hard carbon; XPS: X-ray photoelectron spectroscopy.

organic solvent does not improve the electrochemical characteristics of SIBs. A small quantity of DFEC (0.2%–2% *vol.*) in 1M NaClO₄ + propylene carbonate (PC) decreases both initial CE and capacity retention [Table 1].

Fluorinated dimethyl carbonate (DMCF) was also proposed as an alternative electrolyte additive for SIBs. Fondard *et al.*^[24] concluded that CE [Table 1] decreased with an increase in the amount of DMCF (70% in additive-free electrolyte and 48% and 27% in electrolytes with 1.5% and 3% of DMCF, respectively). The presence of DMCF in the electrolyte results in loss of capacity due to the low voltage pseudo plateau; however, cyclability is higher than in additive-free electrolytes. Chemical characterization of the surface of the HC electrode by XPS at different BE after cycling in NaPF₆ + EC:DMC (1:1) electrolyte with and without

3% *vol.* DMCF shows the appearance of similar compounds [Figure 4D-F] as it was mentioned for electrolytes with FEC additive [Figure 4A-C]. However, the increase of the CO₃ peak (BE ≈ 290 eV) suggests a larger quantity of Na₂CO₃ on the HC surface which could be the reason for the cell capacity decay. It is unfortunate that Fondard *et al.*^[24] did not clearly report the fluorination degree of the DMCF used in this work. According to Yu *et al.*^[76], such a factor could determine the cell performance through additive decomposition routes.

Sulfur-containing Additives

Table 4 listed a few sulfur-containing additives that have been reported for protecting HC anode materials. 1,3-Propane sultone (PS, Table 4) is known as an MIB additive, which reacts with radicals in electrolytes, forming sulfite or sulfate inorganic species^[69]. This additive can also be used to decrease the gas evolution in LiNi_{0.5}Mn_{1.5}O₄/graphite full cells at the state of full charge^[77]. Moreover, it was mentioned that PS can repair broken SEI layers at high temperatures^[78]. Yan *et al.*^[69] found that electrolytes with 3% PS create a SEI layer with a lower impedance and good capacity retention. In recent studies, authors^[59] stated that the reduction peak for PS is observed at 2.02 V *vs.* Na⁺/Na, which means that PS can prevent decomposition of other solvents in the electrolyte. Zhang *et al.*^[59] tested PS as an additive in the electrolyte [1M NaPF₆ + EC/DMC(1/1) + 2% *wt.* FEC], and the results showed that 2% *wt.* PS increased initial CE from 72.3% to 76.7% and capacity retention from 58.7% to 82.0% after 50 cycles in full-cells Na(Ni_{0.4}Mn_{0.4}Cu_{0.1}Ti_{0.1})_{0.999}La_{0.001}O₂/HC full-cells. XPS characterization showed that the electrolytes with PS form ROSO₂Na, RSO₃Na, Na₂SO₃, and Na₂SO₄ on the surface of HC.

Using density functional theory (DFT) calculations, Liu *et al.*^[72] calculated free energies during decomposition of 1,3-Propylene sulfite (1,3-PS, Table 4) through the formation of a 1,3-PS-Na complex, ring opening, and the production of simpler species. Here, reduction reactions are provided:



After ring opening, there are two paths. The first goes through SO₂ gas evolution:



The second path leads to the formation of CH₃CH=CH₂ gas and inorganic Na₂SO₃:



Based on the calculations, the authors^[72,79] concluded that the two-electron reduction of 1,3-PS takes more effort to form Na₂SO₃ compared to the reduction of carbonate esters, such as EC, PC, and vinylene carbonate (VC). But it is easier for a one-electron reduction of 1,3-PS to produce an organic layer on the HC anode compared to EC, PC, and VC.

Che *et al.*^[70] showed that the additive of 1% *wt.* prop-1-ene-1,3-sultone (PES or PST, Table 4) in the electrolyte [1M NaPF₆ + EC/EMC(1/1) + 2% *wt.* FEC] increased capacity retention after 1,000 cycles from 76.6% to 84.4% in pouch cells (NaNi_{1/3}Fe_{1/3}Mn_{1/3}O₂/HC). However, in recent studies, Zhang *et al.*^[59] concluded that increasing the PES amount in the electrolyte [1M NaPF₆ + EC/DMC(1/1) + 2% *wt.* FEC] leads to the formation of a high-resistance SEI layer, so the amount of the additive should not exceed 0.2% *wt.* In any case, even the small amount of PES in the electrolyte worsens the electrochemical performance because the magnitude of SEI impedance (R_{SEI}) and charge transfer impedance (R_{ct}) after 50

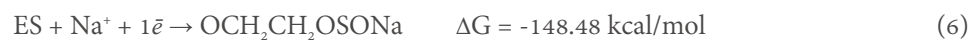
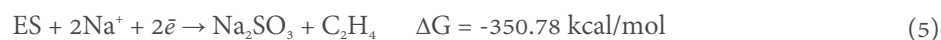
Table 4. Sulfur-containing additives

Chemical name of the additive	1,3-Propane sultone (PS)	1,3-Propylene sulfite (1,3-PS)	Prop-1-ene-1,3-Sultone (PES or PST)	1,3,2-Dioxathiolane-2,2-Dioxide (DTD)	Ethylene Sulfite (ES)
Chemical structure of additive					

cycles is three times greater than that after the first cycle. According to XPS data, PES decomposes both at the cathode and at the anode into several sulfur-containing species (ROSO_2Na , PSO_3Na , and predominantly Na_2SO_3), which consume too many active Na-ions in full-cells. Thus, the PES additive adversely affects the electrochemical performance of the full-cells and their initial CE and capacity retention.

Che *et al.*^[70] claimed that the addition of 1% *wt.* ethylene sulfate or 1,3,2-dioxathiolane-2,2-dioxide (DTD, Table 4) to the electrolyte [1M NaPF_6 + EC/EMC(1/1) + 2% *wt.* FEC + 1% *wt.* PES] increased capacity retention after 1,000 cycles from 84.4% to 92.2% in $\text{NaNi}_{1/3}\text{Fe}_{1/3}\text{Mn}_{1/3}\text{O}_2/\text{HC}$ pouch cells. In another research group, Zhang *et al.*^[59] proved that 2% *wt.* DTD additive in the electrolyte [1M NaPF_6 + EC/DMC(1/1) + 2% *wt.* FEC] improves electrochemical performance of cells [Table 1]: the initial CE increased from 72.3% to 79.1%, and capacity retention after 50 cycles increased from 58.7% to 79.4% in $\text{Na}(\text{Ni}_{0.4}\text{Mn}_{0.4}\text{Cu}_{0.1}\text{Ti}_{0.1})_{0.999}\text{La}_{0.001}\text{O}_2/\text{HC}$ full cells. XPS surface characterization showed that the sample has a strong Na–O–(CO)O–C₂H–R and weak C–C bonds, which means that the DTD additive formed a thick SEI layer, so that is why the signal of the C–C bond of the HC is weak. In addition, DTD formed ROSO_2Na , RSO_2Na , ROSO_3Na , and SO_4^{2-} on the surface of electrodes. It was also observed that 2 *wt.*% FEC additive with 2 *wt.*% DTD synergistically produced more NaF in the SEI film than that with PS or PES.

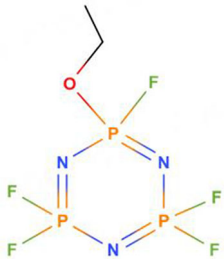
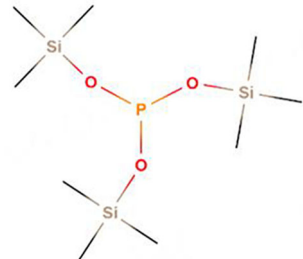
Ethylene sulfite (ES, Table 4) is a well-known effective additive for LIBs; however, Komaba *et al.*^[39] stated that ES shows a detrimental effect in the case of SIBs. Liu *et al.*^[72], using DFT, calculated Gibbs-free energy for decomposition of ES:



Phosphorus-containing Additives

Some phosphorus (P)-containing additives [Table 5] are also listed due to their functionality on the HC anode. Ethoxy(pentafluoro)cyclotriphosphazene (EFPN, Table 5) was first used as a novel flame-retarding additive for LIBs by Xia *et al.*^[80]. In recent years, Feng *et al.*^[61] proposed a non-flammable electrolyte based on EFPN for SIBs. Due to the low dielectric constant of EFPN, the ionic conductivity of the electrolyte with high content of EFPN is low. According to the self-extinguishing time (SET) test, the flammability of the electrolyte decreases with an increase in the content of EFPN [Figure 5A]^[61]. Thus, the most appropriate content of EFPN in the electrolyte is 5% *vol.*

Table 5. Phosphorus-containing additives

Chemical name of the additive	Ethoxy(pentafluoro)cyclotriphosphazene (EFPN)	Tris(trimethylsilyl) phosphite (TMSPi)
Chemical structure of additive		

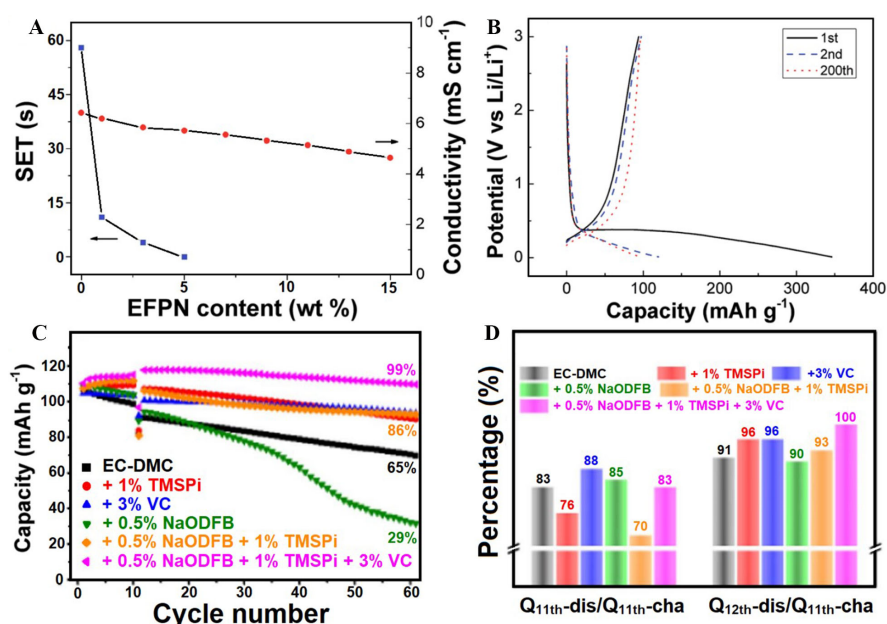


Figure 5. Influence of phosphorus-containing additives: (A) flammability and ionic conductivity of 1M NaPF₆ + EC/DEC (1/1) electrolyte with different amounts of EFPN additive; (B) the 1st, 2nd, and 200th cycles of AB/Na half-cell with 1M NaPF₆ + EC/DEC (1/1) + 5% vol. EFPN electrolyte; Reproduced from ref.^[61], Copyright 2015 RSC; (C) The cycling performances of Na₃V₂(PO₄)₂F₃/C cells with various electrolytes at 55 °C; (D) the percentage of capacity retention and recovery after the self-discharge measurements of Na₃V₂(PO₄)₂F₃/C cells at 100% state of charge for one week. Reproduced from ref.^[68], Copyright 2019 IOP Publishing Limited. DEC: Diethyl carbonate; DMC: dimethyl carbonate; EC: ethylene carbonate; EFPN: ethoxy(pentafluoro)cyclotriphosphazene; NaODFB: sodium (oxalate) difluoro borate; SET: self-extinguishing time; TMSPi: tris(trimethylsilyl) phosphite; VC: vinylene carbonate.

The electrochemical testing of acetylene black/Na half-cells shows a low initial CE [Figure 5B], and the authors claimed that this is due to the decomposition of the electrolyte, which participates in the SEI formation. However, the CE increased in a few cycles to ~100% and remained within 200 cycles [Table 2]. Moreover, the use of EFPN additives decreases the cell resistance and improves cycling performance: capacity retention increased from 78% in an additive-free electrolyte to 97% in an electrolyte with 5% vol. EFPN.

Tris(trimethylsilyl) phosphite (TMSPi, Table 5) has been used as an additive due to its ability to react with an excess of HF, H₂O, O₂, and PF₅ and suppress parasitic reactions on the surface of both the cathode and anode. Leveraging Na₃V₂(PO₄)₂F₃/HC full-cells testing. Cometto *et al.*^[68] concluded that 1% TMSPi, acting as an F⁻ scavenger, produces fluorotrimethyl silane (CH₃)₃SiF in the presence of 0.5% sodium (oxalate) difluoro

borate (NaODFB), which can improve the cell performance [Figure 5].

Other unsaturated chemical compounds as additives

Partially inspired by the success of vinylene carbonate (VC, Table 6), other unsaturated chemical compounds as additives have also drawn substantial attention due to their unique functionalities double or triple bonds, cyclic structures, *etc.*, which could provide a site for polymerization under the reductive condition to modify the SEI. VC is one of the most well-known electrolyte additives for modification of the interphase of the electrodes of LIBs. Komaba *et al.* showed a negative effect of the 2% *vol.* VC on the performance of HC. Further studies^[64] on VC show that a small amount of VC (no more than 0.5% *vol.*) in the electrolyte is enough to produce a robust SEI layer on the electrodes and stabilize them. Bai *et al.*^[64] compared the performance of SIBs with different VC-containing electrolytes (0.5, 1, 5, 10, and 100% by *vol.*) and concluded that the initial CE decreases significantly with an increase of VC concentration [Table 1]. They concluded that HC can retain a reversible capacity of 211 mAh g⁻¹ after 2,000 cycles with an initial CE of 83.0% and a capacity of 221 mAh g⁻¹ during the first cycle in the electrolyte of 1M NaPF₆ + Dimethoxyethane (DME) + 0.5% *vol.* VC. This shows that a lower amount of VC suppresses the continuous decomposition of the electrolyte, which ensures a stable long cycling life of half cells with HC anodes. Earlier full-cell studies^[39] showed that VC-added electrolytes have a decreased reversible capacity and initial CE [Table 1]; however, other studies showed that a lower amount of VC improved the characteristics of full-cells, which made VC more useful in practical applications^[64].

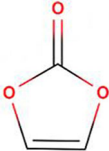

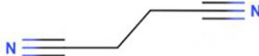
Bai *et al.*^[64] analyzed the surface of cycled HC electrodes by XPS. The results showed that the carbonate group peak (Na₂CO₃ and/or RCO₃Na) is much stronger in VC-containing electrolytes. Moreover, it was noticed that VC could be reduced to polymeric species, such as -(OCO₂CH=CH)_n- and -(CHOCO₂CH)_n-, during the process of SEI formation. Liu *et al.*^[72] carried out DFT calculations to understand various reduction routes of VC as below:



Succinic anhydride (SA, Table 6) is an organic compound with a ring and a formula of (CH₂CO)₂O. Kim *et al.*^[63] assembled HC/HC symmetric cells to estimate their electrochemical behavior in the electrolyte of 1M NaPF₆ + EC/ diethyl carbonate (DEC) (1/1) with 0.5 *wt.*% SA. It was stated that 0.5 *wt.*% is the optimum amount for SA additives. It also has been reported^[63] that the addition of SA can improve the cell performance at both 25 °C [Table 1] and 60 °C with a lower resistance, which is caused by the modified SEI. According to the XPS data^[63], the addition of SA leads to the formation of a higher amount of Na₂CO₃ and Na alkyl carbonates in the SEI of the HC anode.

Succinonitrile (SN, Table 6) is an organic solvent with a strong triple bond (-C≡N), which is known as a SEI-forming additive for MIBs. As reported by Yan *et al.*^[69], using the SN additive (1 *wt.*%) alone within the electrolyte of 1M NaPF₆ + EC/PC (1/1) increases the resistance of Na₃V₂(PO₄)₂F₃/HC full-cells and causes a high irreversible capacity during the first cycle (40 mAh g⁻¹ vs. 27 mAh g⁻¹ for the additive-free electrolyte). However, this SN additive can contribute to the cell performance improvement at a high temperature by decreasing the self-discharge and retaining the capacity retention when it is used as a part of blended electrolyte additives (*i.e.*, with NaODFB, PS, and VC additives)^[69].

Table 6. Other unsaturated chemical compounds as additives

Chemical name of the additive	Vinylene carbonate (VC)	Succinic Anhydride (SA)	Succinonitrile (SN)
Chemical structure of additive			

Ionic additives

In addition to molecular compounds, ionic compounds (salts, Table 7) were reported to participate in the SEI formation, with either cation or anion. Trisaminocyclopropenium perchlorate (TAC·ClO₄) is an organic salt that is used for SIB systems as an additive for overcharge protection. This additive for Na₃V₂(PO₄)₃/HC full cells was described for the first time by Ji *et al.*^[81] This group showed that the addition of 0.1M TAC·ClO₄ to 1M NaClO₄ + EC/DMC (1/1) does not affect the initial CE of HC (71.2% in the base electrolyte and 72.4% in TAC-added electrolyte). Moreover, the Na₃V₂(PO₄)₃/HC full-cell showed a strong anti-overcharging ability during 176 cycles at a 0.5C rate with 100% overcharge.

RbPF₆ and CsPF₆ [Table 7] are used as a source of Rb⁺ and Cs⁺ ions, which were proposed as electrolyte additives for HC anodes in SIBs. Che *et al.*^[65] compared electrochemical performance of Na/HC cells in an electrolyte of 0.8M NaPF₆ + EC/PC (1/1) + 2% FEC with and without 0.05M RbPF₆ or CsPF₆. It was noticed that the presence of the Rb⁺ and Cs⁺ ions improves the cell lifetime [Table 2] by showing a higher initial CE, decreasing the cell impedance, and maintaining a higher capacity retention. XPS characterization of the SEI layer showed that Rb⁺ and Cs⁺ ions increase the content of P–F or C–F components and decrease the number of organic species of C=O, C–F, and C–O–C(R₁) [Figure 6].

Sodium metal anode

A sodium metal anode has a high specific capacity (1165 mAh g⁻¹) and a lower potential than many other anode materials; however, metallic sodium can actively react with electrolyte components, which leads to side reactions, a thicker SEI, and a high impedance. Especially sodium dendrite will form and grow during cell cycling, which could cause multiple safety issues.

Ionic additives

Many ionic additives have been reported to improve the sodium metal reversibility by tuning the SEI composition and even forming an alloy layer to homogenize the Na deposition behavior. Tin chloride (SnCl₂, Table 8) is an inorganic compound that is used as an additive for SIBs. Zheng *et al.*^[82] reported that SnCl₂ can react with sodium metal to form a Na–Sn alloy. At the same time, Cl⁻ anion participates in the formation of NaCl in the SEI. XPS data showed that the SEI consisted of NaOH, Na₂CO₃, ROCO₂Na, NaCl, and Na–Sn alloy layers on the surface of metallic sodium. Thus, 50 mM SnCl₂ can maintain a stable overpotential for a Na/Na symmetric cell during more than 500 h of cycling. Sodium polysulfide (Na₂S₆, Table 8) was reported by Wang *et al.*^[83] as a pre-passivation additive for SIBs with sodium metal anodes. Due to the decomposition of Na₂S₆, the SEI layer consists of several inorganic compounds (Na₂O, Na₂S₂, and Na₂S), which results in a stable operation of SIBs. Antimony trifluoride (SbF₃, Table 8) is an inorganic compound, which was introduced as an additive by Fang *et al.*^[84] They tested Na₃V₂(PO₄)₃/Na cells in a high concentration electrolyte of 4M sodium bis-(fluorosulfonyl)imide (NaFSI)/DME with 1% SbF₃. They stated that a bilayer-structure SEI appears with a Na–Sb alloy and NaF-rich inorganic compounds during cell cycling, which was confirmed by energy dispersive X-ray spectroscopy (EDS) mappings [Figure 7A].

Table 7. Ionic additives

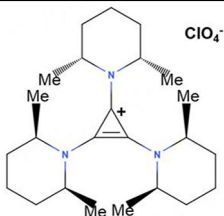
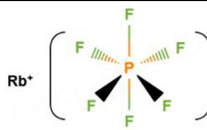
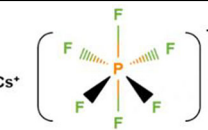
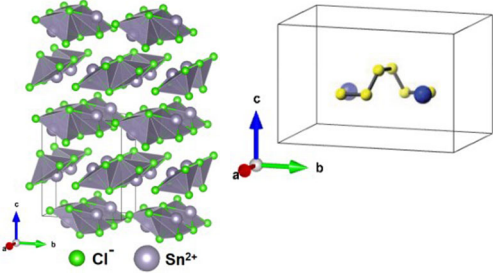
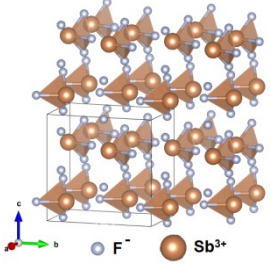
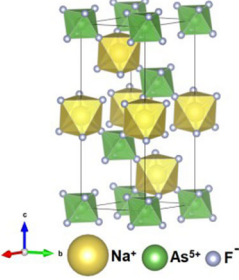
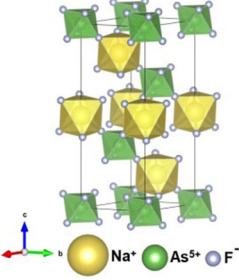
Chemical name of the additive	Trisaminocyclopropenium perchlorate (TAC-ClO ₄)	RbPF ₆	CsPF ₆
Chemical structure of additive			

Table 8. Ionic additives

Chemical name of the additive	Tin Chloride (SnCl ₂)	Sodium Polysulfide (Na ₂ S ₆)	Antimony trifluoride (SbF ₃)	Sodium Hexafluoroarsenate (NaAsF ₆)
Chemical structure of additive				

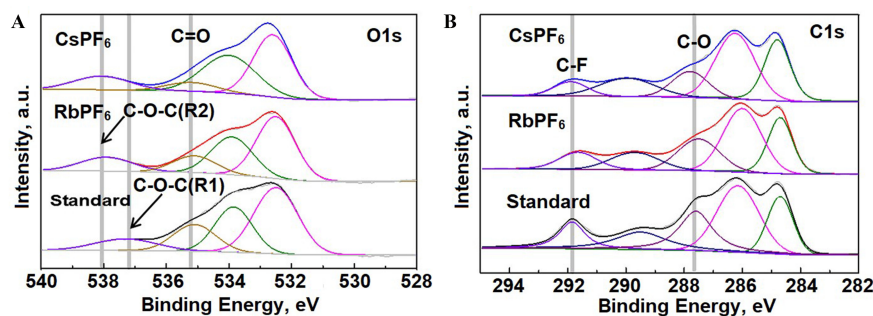


Figure 6. XPS spectra of HC electrodes after three cycles in different electrolytes (A) O 1s and (B) C 1s. Reproduced from ref^[65], Copyright 2017 Elsevier. HC: Hard carbon; XPS: X-ray photoelectron spectroscopy.

Moreover, according to XPS spectra, there are different products due to the decomposition of carbonate electrolytes (Na₂CO₃, ROCO₂Na, *etc.*). SbF₃ additives also improve the stability of metallic sodium without increasing the polarization of symmetric cells [Figure 7B]. With the addition of SbF₃, the impedance of the cell was decreased from 643.1 Ω to 9.3 Ω [Figure 7C and D]. Thus, electrolytes with SbF₃ additives exhibit an outstanding effect in stabilizing the surface of metallic sodium and improving the electrochemical characteristics of cells.

Sodium hexafluoroarsenate (NaAsF₆, Table 8) was found by Wang *et al.*^[85] as an effective SEI-film forming additive for SIBs with metallic Na anodes. The addition of 0.75 wt.% NaAsF₆ to 1M NaTFSI with FEC can stabilize the Na/Al cell over 400 cycles and Na/Na symmetric cells for more than 350 h. XPS data showed that NaAsF₆ additives helped to form a NaF-rich SEI with O-As-O polymer species. Thus, a trace amount of NaAsF₆ can stabilize the surface of sodium metal anodes.

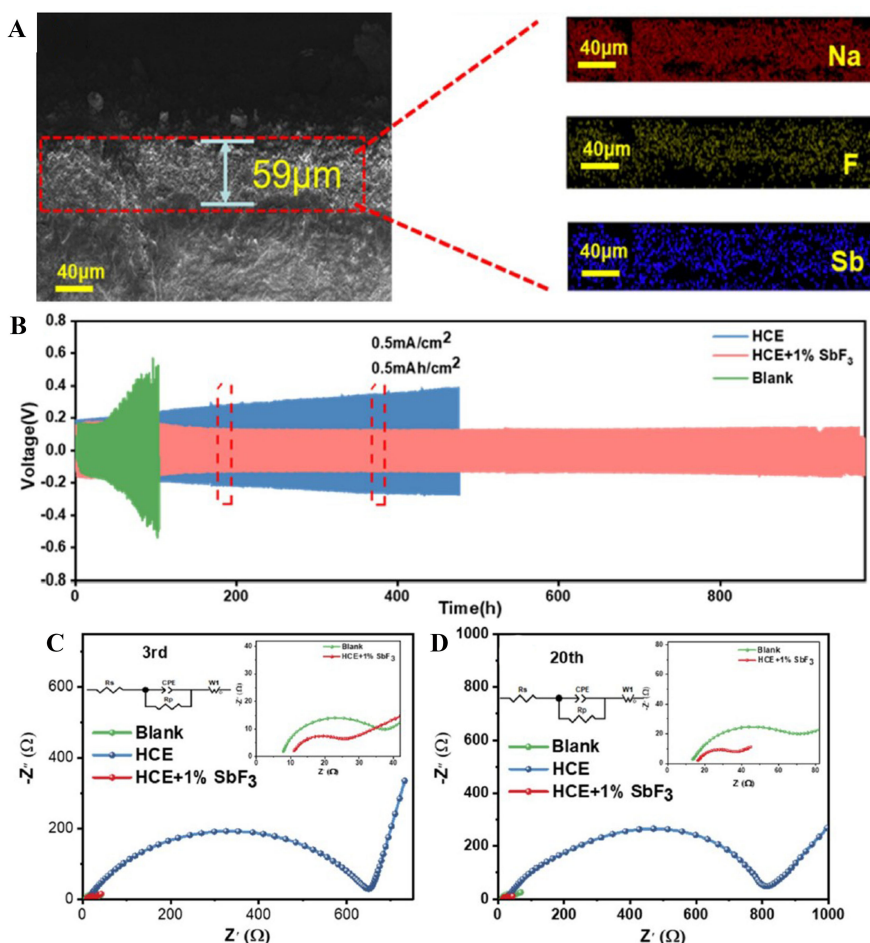


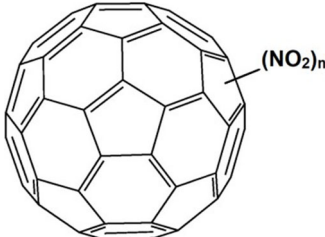
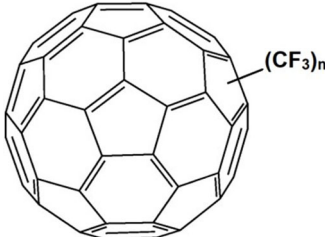
Figure 7. Electrochemical performance of cells with SbF₃ additive. (A) Cross-sectional SEM and EDS mappings of cycled Na metal in the electrolyte with 1% SbF₃ additive; (B) Testing in symmetric Na||Na cells. Nyquist plots for Na₃V₂(PO₄)₃/Na cells with different electrolytes after (C) three cycles and (D) 20 cycles. Reproduced from ref^[84], Copyright 2020 Elsevier. EDS: Energy dispersive X-ray spectroscopy; SEM: scanning electron microscopy.

Fullerene-containing additives

Fullerene (C₆₀) cages have been reported to preferentially anchor on the sodium surface to induce uniform Na deposition^[86,87]. With the addition of special functional groups on the C₆₀ cages, those additives are able to further improve the reversibility of sodium metal anodes. Nitrofullerene [C₆₀(NO₂)₆, Table 9] was first proposed as an additive for LIBs by Jiang *et al.*^[86] Recently, this additive was reported as a highly electrolyte compatible additive for SIBs. Li *et al.*^[87] showed that C₆₀(NO₂)₆ is compatible with different solvents (PC, FEC, DEC, DMC, EMC, DME, triglyme, and diglyme). Moreover, the additive improves the stability of sodium metal by maintaining a constant overpotential [Figure 8A] and reducing the interface resistance and charge transfer resistance [Figure 8B] of symmetrical cells. XPS spectra [Figure 8C] showed that the addition of C₆₀(NO₂)₆ forms three new species on the surface of the electrode: C₆₀, NaN_xO_y, and Na₃N, which can protect the electrolyte from further decomposition on the electrode surface. C₆₀(NO₂)₆ also can improve the Na₃V₂(PO₄)₃/Na cell lifetime [Figure 8D].

Trifluoromethylfullerene [C₆₀(CF₃)₆, Table 9] was described as a new additive for SIBs by Li *et al.*^[88]. They concluded that C₆₀(CF₃)₆ can enhance Na⁺ migration in the electrolyte, form a NaF-rich SEI, and improve the cycling performance and rate capabilities. Overpotential maintained a constant value within over

Table 9. Fullerene-containing additives

Chemical name of the additive	Nitrofullerene [$C_{60}(NO_2)_6$]	Trifluoromethylfullerene [$C_{60}(CF_3)_6$]
Chemical structure of additive		

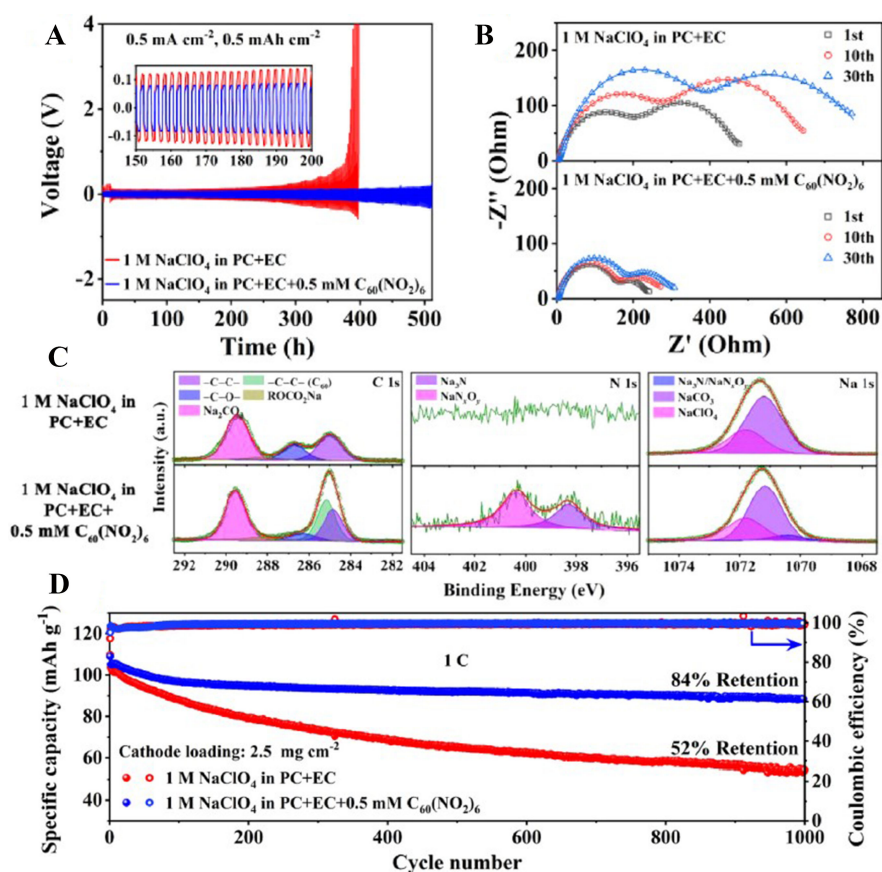


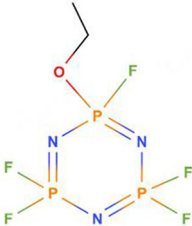
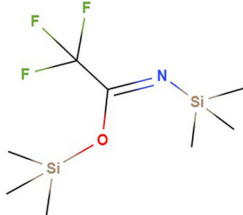
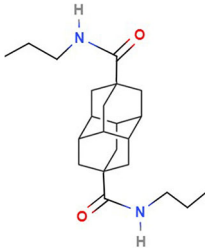
Figure 8. The effect of $C_{60}(NO_2)_6$ additives on sodium metal anodes. (A) cycling performance of and (B) Nyquist plots for the Na/Na symmetric cells; (C) XPS spectra of cycled Na; (D) cycling performance of $Na_3V_2(PO_4)_3/Na$ cells. Reproduced from ref^[87], Copyright 2021 Elsevier. EC: Ethylene carbonate; PC: propylene carbonate; XPS: X-ray photoelectron spectroscopy.

1,200 h in Na/Na symmetric cells. According to XPS spectra, the SEI layer has a higher NaF and C_{60} content in the electrolyte with $C_{60}(CF_3)_6$ additives because it is more favorable for $C_{60}(CF_3)_6$ to decompose compared to $NaPF_6$ or DME solvent. Thus, C_{60} and CF_3 groups can significantly improve the electrochemical performance of cells with sodium metal anodes.

Nitrogen-containing additives

EFPN [Table 10] is an organic compound that was proposed^[61] as an additive for non-flammable electrolytes for SIBs. This compound and its characteristics were described in this review previously as an

Table 10. Nitrogen-containing additives

Chemical name of the additive	Ethoxy(pentafluoro)cyclotriphosphazene (EFPN)	Acetamide (N, O-bis(trimethylsilyl) trifluoroacetamide (BSTFA)	Diamondoid (bis- <i>N,N'</i> -propyl-4,9-dicarboxamidediamantane (DCAD)
Chemical structure of additive			

additive for carbonaceous anode additives. Compatibility testing of the EFPN with metallic sodium showed no reactions. Oxidation current starts at 4.8V *vs.* Na/Na⁺ for 5% EFPN-added electrolyte in coin cells with Na/stainless steel electrode.

Acetamide (N, O-bis(trimethylsilyl) trifluoroacetamide (BSTFA, Table 10) was found by Jiang *et al.*^[89] as a promising additive for SIBs with a sodium metal anode. The main purpose of this additive is to scavenge HF and H₂O. This additive was introduced into an ultra-low concentrated electrolyte of 0.3M NaPF₆ + EC/PC (1/1) to improve Na₃V₂(PO₄)₃/Na cells. 2 wt.% BSTFA decreases the impedance of Na/Na symmetric cells and keeps it constant even after 100 h of cycling. BSTFA helps to protect the sodium metal anode from dendrite growth by creating a uniform and dense SEI. Moreover, this additive improves the electrochemical performance by decreasing impedance and increasing capacity retention and CE of the Na₃V₂(PO₄)₃/Na cells.

Bis-*N,N'*-propyl-4,9-dicarboxamidediamantane (DCAD, Table 10) was used as an additive to avoid the dendrite formation in SIBs with a sodium metal anode. Kreissl *et al.*^[90] showed that 2.5 mg/mL of DCAD improves the performance of Na/Na symmetric cells and Na/O₂ cells by stabilizing the surface of metallic sodium.

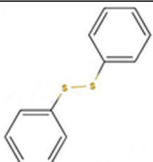
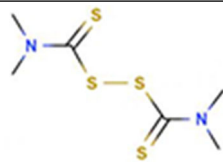
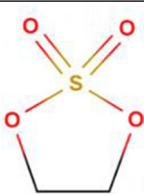
Sulfur-containing additives

Sulfur-containing electrolytes were found to improve the sodium metal anode reversibility by forming sulfur-containing SEI species (e.g., Na₂S, Na₂SO₃). Diphenyl disulfide (DPDS, Table 11) is an organic compound with a structure of di-Ph-S, which was tested by Zhu *et al.*^[91] as an additive to form a stable SEI film and suppress the dendrite growth. They showed that an addition of 1% DPDS additive can maintain a stable overpotential of Na/Na symmetric cells for more than 200 h of cycling. SEM data showed that DPDS decomposes to Ph-S-Na and participates in the formation of a uniform and smooth SEI layer. Moreover, Prussian blue/Na cells show a stable cycling performance with a 1% DPDS additive.

Tetramethylthiuram disulfide (TMTD, Table 11) was investigated by Zhu *et al.*^[92] as a film-forming additive with organic sulfide salts. It was stated that the overpotential of Na/Na symmetric cells remains stable for 600 h of cycling in an electrolyte with 2 wt.% TMTD. Moreover, the electrolyte with 2 wt.% TMTD improved the electrochemical performance of Prussian blue/Na full-cells with a high CE of 94.25% and capacity retention of 80% after 600 cycles at 4C-rate.

DTD [Table 11] was used by Zhu *et al.*^[93] as an additive to form an SEI with the function of preventing sodium dendrite growth. Na/Na symmetric cells keep a stable performance for > 1,350 h of cycling in an

Table 11. Sulfur-containing additives

Chemical name of the additive	Diphenyl disulfide (DPDS)	Tetramethylthiuram disulfide (TMTD)	Ethylene sulfite or 1,3,2-dioxathiolane-2,2-dioxide (DTD)
Chemical structure of additive			

electrolyte with a 5% DTD additive. They stated that the synergistic effect of two additives, FEC and DTD, in trimethyl phosphate (TMP)-containing electrolytes can form a SEI layer consisting of Na_2S , Na_2SO_3 , NaF , and Na_3PO_4 , which helps to avoid further electrolyte and electrode degradation. In addition, TMP-FEC-DTD electrolytes can increase capacity retention and CE of Prussian blue/Na cells.

Other unsaturated chemical compounds as additives

A few other common unsaturated additives have also been reported to modify the SEI of sodium metal anodes, thus improving its lifetime. In the electrolytes with FEC [Table 12], the passivation of metallic sodium can be improved, which suppresses side reactions between Na and other electrolyte components. Komaba *et al.*^[39] assumed that almost all polar organic solvents are not thermodynamically stable at ~ 0 V vs. Na^+/Na , but FEC as an additive can help to achieve the highly reversible Na plating. Rodriguez *et al.*^[94] tested 1M NaPF_6 + PC/FEC (98/2) and claimed that FEC improves the electrochemical performance and helps to form a NaF-rich SEI but leads to gas evolution and dendrite formation, which, in turn, leads to poor contact between electrodes and more safety concern. However, according to many other reports^[63,94-98], the presence of FEC in electrolytes showed improvements of electrochemical performance with a stabilized SEI, which helps to avoid permanent electrolyte degradation on the electrode surface.

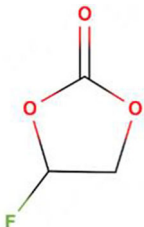

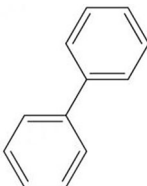
SA [Table 12] has already been described previously in the section of additives for carbonaceous anodes. Fan *et al.*^[99] concluded that SA participates in the formation of CEI/SEI in half-cells and improves the electrochemical behavior in electrolytes with FEC. Kim *et al.*^[63] stated that SA forms a more resistive SEI but suppresses the dendritic growth on the sodium metal anode.

Biphenyl (BP, Table 12) is an organic aromatic compound consisting of two benzene rings connected by a covalent bond. BP is a well-known additive for the overcharge protection in LIBs, so Feng *et al.*^[100] tested 1M NaPF_6 + EC/DEC (1/1) electrolyte with and without BP. They claimed that a BP-added electrolyte starts to oxidize at 4.3V vs. Na/Na^+ , during which the BP molecules are electropolymerized on the electrode surface with H_2 production. This can be seen from the experiment on the cell overcharging process [Figure 9A and B]. It was also claimed that products of BP decomposition can increase the impedance of a cell [Figure 9C]. Moreover, the presence of 3% BP in electrolytes does not affect the electrochemical performance of the cell [Figure 9D].

Alloy anode

Sodium metal alloys can be formed when the Na^+ inserts into the metal alloys with alloying reactions. Unlike carbon-based anodes, an alloy-based anode suffers from a rapid volume expansion during cycling, leading to the SEI cracking accompanied by continuous parasitic reactions to re-establish the SEI layer. Although tin (Sn) and antimony (Sb) are proposed as promising anode materials for SIBs with a high theoretical specific capacity (847 mAh g^{-1} for Sn, 610 mAh g^{-1} for Sb), their unstable SEI and big volume expansions compromise their reversibility during cycling.

Table 12. Other unsaturated chemical compounds as additives

Chemical name of the additive	Fluoroethylene carbonate (FEC)	Succinic anhydride (SA)	Biphenyl (BP)
Chemical structure of additive			

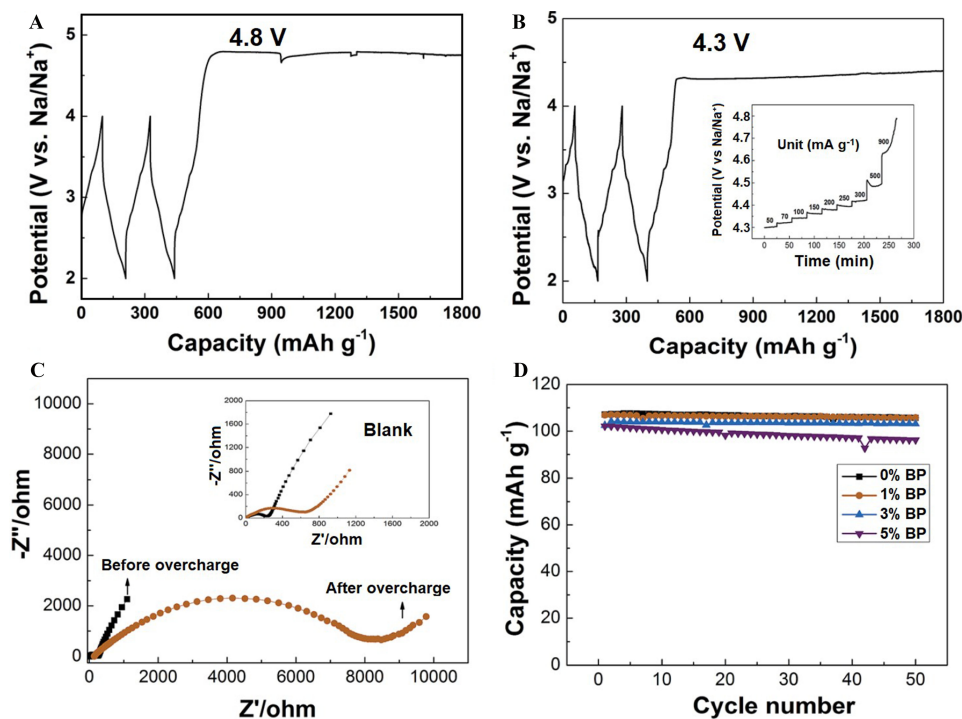


Figure 9. Electrochemical testing for $\text{Na}_{0.44}\text{MnO}_2/\text{Na}$ cells in electrolyte (A) without BP and (B) with 3% BP; (C) the impedance before and after cell overcharging with 3% BP; (D) cycling performance with different BP amount in the electrolyte at 50 mA g^{-1} between 2 and 4 V. Reproduced from ref^[100], Copyright 2015 RSC publication. BP: Biphenyl.

FEC is recognized as the most efficient electrolyte additive that can improve the lifetime of Sn and Sb anodes [Table 13]^[101-111]. Many researchers^[95,101-111] stated that FEC additive improves capacity retention, rate capabilities, and CE because a stable SEI layer can be formed to prevent the electrolyte degradation. Qian *et al.*^[110] showed that 5% FEC can form a stable SEI with constant resistance. Without the FEC additive, SEI films become denser and more inhomogeneous during cycling. Herein, we summarize the influence of FEC additives on the electrochemical performance of Sn- and Sb-based alloy anode materials in [Table 13].

FEC is the most well-known additive for extending the lifetime of P anodes. Yabuuchi *et al.*^[113] showed that FEC can improve the electrochemical performance and stabilize the reversible capacity of P anodes. They found that FEC can create some F-containing species, such as NaF and $\text{Na}_x\text{PF}_y\text{O}_z$, which can stabilize the SEI of Na_xP anodes and prevent further electrolyte decompositions. A high efficiency of the FEC additive was confirmed by the research of Dahbi *et al.*^[114]. They showed that the reversible capacity of the cell is able

Table 13. The electrochemical performance of Sn- and Sb-based alloy anodes in different electrolytes with the FEC additive

Anode	Salt	Solvent	Additive	ICE, %	C _p , mAh/g	C _r , mAh/g	N	Ref.
AlSb	1M NaClO ₄	PC	-	-	450	90	15	Baggetto <i>et al.</i> , 2013 ^[101]
			5% vol. FEC	-	440	210	50	
Ge			-	-	340	30	50	Baggetto <i>et al.</i> , 2013 ^[102]
			5% vol. FEC	-	280	50	150	
Mo ₃ Sb ₇			-	-	330	20	100	Baggetto <i>et al.</i> , 2013 ^[103]
			5% vol. FEC	-	330	150	100	
Sb			-	65	544	14	100	Darwiche <i>et al.</i> , 2012 ^[104]
			5% vol. FEC	76	537	576	100	
SnSb			5% vol. FEC	59	536	506	100	Ma <i>et al.</i> , 2018 ^[105]
SnSb/C		EC/PC (1:1)	-	75	475	105	30	Kim <i>et al.</i> , 2014 ^[106]
			2% vol. FEC	77	610	110	30	
SnSb/TiC/C			-	70	300	200	30	
			2% vol. FEC	66	260	170	70	
FeSb/TiC/C			-	60	215	90	100	Kim <i>et al.</i> , 2014 ^[107]
			2% vol. FEC	57	205	204	100	
Cu ₆ Sn ₅ /TiC/C			-	61	225	90	100	Kim <i>et al.</i> , 2015 ^[108]
			2% vol. FEC	56	146	155	100	
Sn/C			-	70	445	20	20	
Sn/CNF		EC/DMC (1:1)	-	68	280	60	45	Sadan <i>et al.</i> , 2017 ^[109]
			5% vol. FEC	45	270	155		
Sb/C	1M NaPF ₆	EC/DEC (1:1)	-	85	610	0	100	Qian <i>et al.</i> , 2012 ^[110]
			5% vol. FEC	85	611	575	100	
SnSb/CNF			-	57	380	130	200	Ji <i>et al.</i> , 2014 ^[111]
			5% vol. FEC	53	347	345	200	
Sn/CNF		EC/DMC (1:1)	-	24	150	70	45	Sadan <i>et al.</i> , 2017 ^[109]
			5% vol. FEC	30	230	185		
Sn/CNF	1M NaCF ₃ SO ₃	EC/DMC (1:1)	-	50	325	100	45	Sadan <i>et al.</i> , 2017 ^[109]
			5% vol. FEC	16	135	135		
Sn/CNF	1M NaBF ₄	EC/DMC (1:1)	-	58	270	80	45	Sadan <i>et al.</i> , 2017 ^[109]
			5% vol. FEC	8	60	60		

P, including three allotropic forms: white, red, and black, is another promising anode material for SIBs with a high theoretical specific capacity (2,596 mAh g⁻¹). However, the low electronic conductivity (10⁻¹⁴ S cm⁻¹) and the following difficulty in the formation of a stable and smooth SEI on the surface are the main problems of using P as an anode material. Among P anodes, the most stable forms are red and black, which can be prepared by heating under high pressure. Many studies^[112-117] on P are devoted to upgrading its structure, and the issue of electrolyte additives is rarely covered. This review will be dedicated only to electrolyte additives to improve the stability of SEIs on the P anode surface. CNF: Carbon nano-fibers; DEC: diethyl carbonate; DMC: dimethyl carbonate; EC: ethylene carbonate; FEC: fluoroethylene carbonate; ICE: initial coulombic efficiency; PC: propylene carbonate; SEI: solid electrolyte interphase; SIBs: sodium-ion batteries.

to reach 1,587 mAh g⁻¹ with a high initial CE. Moreover, the electrode surface is more uniform and thinner with FEC, according to SEM images. VC has also been reported to improve the electrochemical performance of P anodes. Dahbi *et al.*^[114] stated that 1% VC additive forms a homogeneous SEI layer on P anodes and improves the electrochemical performance. The main components of the SEI layer in VC-containing electrolytes are -OCO₂Na groups and polymeric chains. Thus, VC additives can stabilize the SEI layer and help to achieve a long-cycling life of cells with P anodes. Table 14 summarizes the effect of FEC and VC on the electrochemical performance of P anode materials.

Table 14. The electrochemical performance of phosphorus anodes in different electrolytes

Electrolyte	Additive	CE at the 1st cycle, %	Discharge capacity at the 1st cycle, mAh/g	Discharge capacity at the <i>n</i> th cycle, mAh/g	Number <i>n</i> of cycles	Ref.
1M NaPF ₆ + EC/DEC (1:1)	-	72.0	1,479	957	23	Dahbi <i>et al.</i> , 2016 ^[114]
	5% vol. FEC	75.0	1,587	1,458		
	1% vol. VC	76.3	1,615	1,484		
	10% vol. FEC	75.6	1,183	648	100	Li <i>et al.</i> , 2018 ^[115]
	10% vol. FEC	72.0	1,354	1,191	100	Capone <i>et al.</i> , 2019 ^[117]
	5% vol. FEC	71.8	1,786	972	100	Zhang <i>et al.</i> , 2020 ^[112]
1M NaClO ₄ + EC/PC (1:1)	5% vol. FEC	98.7	985	854	100	Song <i>et al.</i> , 2023 ^[116]

DEC: Diethyl carbonate; EC: ethylene carbonate; FEC: fluoroethylene carbonate; PC: propylene carbonate; VC: vinylene carbonate.

Other anodes (Metal Oxides/Sulfides, Organic Materials)

In addition to the anode materials discussed above, there are other choices of anodes for SIBs, which are being developed with various Na⁺ ion storage mechanisms (e.g., conversion, intercalation). In specific, the majority of TM oxides or sulfides (e.g., Fe₂O₃^[118], MoS₂^[119]) electrochemically react with Na⁺ ions through conversion reactions, while several Ti-based compounds (e.g., TiO₂^[120], Na₂Ti₃O₇^[121]) are able to allow Na⁺ ion intercalations. Additionally, organic materials, especially primary conjugated carbonyl-based compounds^[122,123] and Schiff base polymers^[124,125], have also been investigated as anodes for SIBs due to their low cost and abundant natural resources.

However, the research activities on these anode materials for SIBs have been focused on the development of electrode materials, and the investigation into the effects of electrolyte additives is still in its infant stage, with few literature reports. There is plenty of room in the area of electrolyte additives to improve the performance of these anodes from the perspective of lifetime, safety, and gas suppression.

ELECTROLYTE ADDITIVES FOR IMPROVING CATHODE PERFORMANCE

Substantial efforts have been devoted to improving the performance of cathodes by tuning their chemistries and structure, as the “best choice” for the cathode active material is still under debate. Currently, the most promising cathode materials for SIBs include layered TM oxides (Na_xTMO₂), Prussian white/blue, polyanion, and organic materials^[7]. However, there are fewer reports available regarding the chemical composition and formation mechanisms of the CEI due to complicated cathode surface reactions and complex responses to air exposure. Similar to LIB cathodes, the operating potential of most SIB cathode materials does not depart too much from the oxidation stability limits of the electrolyte components. Therefore, there have been limited efforts to develop electrolyte additives and understand their effects on CEI stability as compared to the efforts spent on anode interphases.

Leveraging references specifically studying the CEI of SIBs, we discuss the additives according to their effects on cell performance, including cell lifetime and safety. Most cathode additives discussed here are the same as the ones used for anode materials, so their chemical structures will not be shown in this section.

Additives for extending cell lifetime

SIBs continue to face challenges such as voltage and capacity fading over time. In particular, cathodes in a charged (de-sodiated) state have been investigated as the main source of cell degradation during cycling,

especially when side reactions are caused by trace amounts of water. To extend the lifetime of SIBs, a robust CEI with minimum moisture is necessary to prevent parasitic reactions between cathode materials and electrolytes. This work discusses cathode additive studies aimed at improving the lifetime of SIBs from the perspective of CEI formation and water scavenging, respectively.

Function on CEI formation

Single additive

FEC is one of the most commonly used functional electrolyte additives in extending the lifetime of SIBs, largely due to its ability to compositionally and structurally improve the CEI^[126]. Several case studies demonstrate the positive role of FEC with various cathode chemistries. For instance, FEC contributes to the increased formation of NaF as the inorganic passivation layer, which suppresses the TM dissolution and cathode structural transformation in the NaFeO₂ cathode [Figure 10A]^[20]. Such behavior has been observed with 5 wt.% FEC and Na₂FeP₂O₇ cathode material, in which a specific capacity of 81 mAh g⁻¹ after 500 cycles was achieved, compared to only 31 mAh g⁻¹ without FEC^[127]. In the report of Lee *et al.*^[128], several linear carbonate-containing electrolytes were compared with 5 wt.% FEC additives using the Na₄Fe₃(PO₄)₂(P₂O₇) cathode. One such combination included 0.5 M NaClO₄ in EC:PC:DEC (5:3:2, by vol.) with 5 wt.% FEC and showed an improvement in both cyclability and specific capacity compared to a reference electrolyte. XPS results confirmed the presence of a NaF-containing protective layer, which is believed to have contributed to cell stability and the suppression of DEC decomposition. On a more mechanistic level, Cheng *et al.* demonstrated that 3% vol. FEC promotes the formation of NaF-enriched species on P2-Na_xCo_{0.7}Mn_{0.3}O₂ cathodes in the electrolyte of 1M NaClO₄ in PC [Figure 10B], which was confirmed with XPS^[129]. In addition to fluorinating the CEI, FEC has also been shown to structurally change the interphase. TEM and XPS analysis by Wu *et al.*^[130] showed that the use of FEC with Na_{2/3}Ni_{1/3}Mn_{2/3}O₂ cathodes fluorinated the CEI and decreased its thickness from approximately 43 nm to 8 nm, thereby generating a more compact and stable CEI to prevent an excessive electrolyte decomposition [Figure 10C].

Another commonly used electrolyte additive, VC, can enhance the performance of a SIB by modifying the structure and composition of CEI. As reported by Shi *et al.*^[131] [Figure 11A and B], the addition of VC additives into 1 M NaCF₃SO₃⁻ diglyme (DGM) electrolyte with a Na₃V₂(PO₄)₃@C cathode allowed the VC to oxidize with DGM to form a more consecutive and uniform CEI layer that prevented electrolyte degradation. With FeS as an anode, the full-cell showed a promising capacity retention of 67% after 1,000 cycles. VC was used with a Na₃V₂(PO₄)₃ cathode in 1.2 M NaTFSI-TMP/bis(trifluoromethanesulfonyl)imide (BTFE) electrolyte to help create a stable, fire-retardant SIB [Figure 11C]^[132]. XPS and SEM results indicated that VC played a role in forming a more stable and homogenous organic-inorganic CEI rather than one saturated with organic compounds. Adding the proper amount of an additive is critical to optimize the electrochemical performance. It was reported by Law *et al.* [Figure 11D] that utilizing 5% vol. VC with a Na₂MnSiO₄ cathode material generated a “meta-stable passivation film” on the cathode that suppressed Mn dissolution and lowered the cell impedance^[133]. VC, with the addition of lower than 5% vol., did not provide a thick or stable enough passivation layer, while percentages higher than 5% vol. created a resistant and thick interphase.

Dinitriles have been proposed as electrolyte additives and solvents due to their decent thermal and electrochemical stability^[134]. Song *et al.*^[135] assessed the effectiveness of adiponitrile (ADN) as an additive for SIBs using the Na_{0.76}Ni_{0.3}Fe_{0.4}Mn_{0.3}O₂ cathode at different temperatures and with various percentages of ADN. TEM and XPS analyses demonstrated the addition of 3 wt.% ADN helped form a compact and uniform CEI layer [Figure 12A] containing NaF- and NaCN-rich complexes. These inorganic compounds

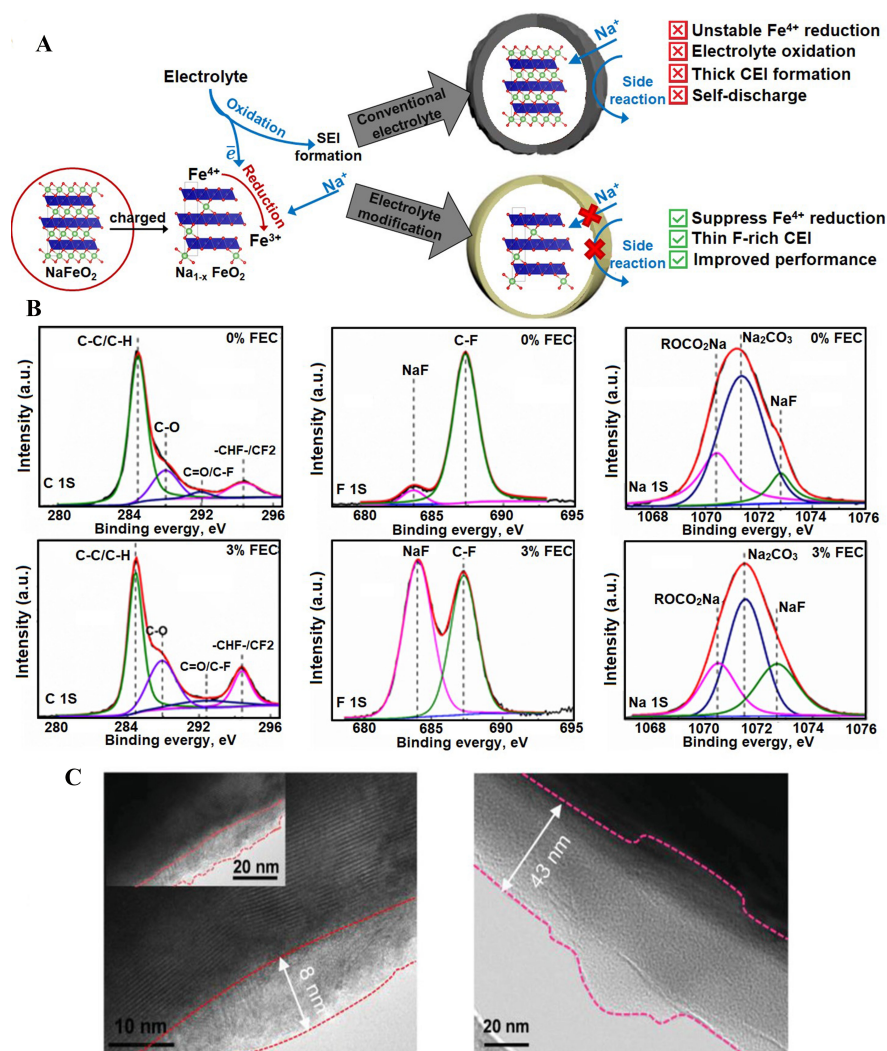


Figure 10. The effect of FEC on SIB cathodes. (A) Interfacial degradation mechanism of the NaFeO₂ cathode, Reproduced from ref.^[20], copyright 2022 IOP Publishing; (B) Na 1s XPS profiles of P2-Na_xCo_{0.7}Mn_{0.3}O₂ cathodes after 20 cycles in electrolyte with and without FEC, Reproduced from ref.^[129], Copyright 2019 Acta Physico-Chimica Sinica publication; (C) TEM images of Na_{2/3}Ni_{1/3}Mn_{2/3}O₂ cathodes cycled in FEC electrolytes and PC electrolytes characterizing the CEI layer, Reproduced from ref.^[130], copyright 2021 Wiley. CEI: Cathode electrolyte interphase; FEC: fluoroethylene carbonate; PC: propylene carbonate; SEI: solid electrolyte interphase; SIB: sodium-ion battery; TEM: transmission electron microscopy; XPS: X-ray photoelectron spectroscopy.

inhibited side reactions and ensured a charge balance at the cathode surface. With a more effective CEI, the ADN-containing SIB showed increased discharge capacities of 10.5%, 8%, and 13% at operating temperatures of 45 °C, -10 °C, and -20 °C, respectively. Additionally, these cells delivered capacity retention of 78% after 220 cycles compared to a cell without ADN additive, which dropped to 75% capacity after 40 cycles.

Sulfur-containing additives have been pursued, similar to other singular additives such as FEC, due to their ability to form stable CEIs and prevent the decay of cells^[136]. PS was used as an additive along with FEC as the co-additive in an attempt to create stable interphases with multifunctional gel polymer electrolyte^[137]. A thinner and more stable CEI layer with PS decomposition products was observed on the surface of the graphite cathode, which prevented electrolyte decomposition. In another experiment that combined several

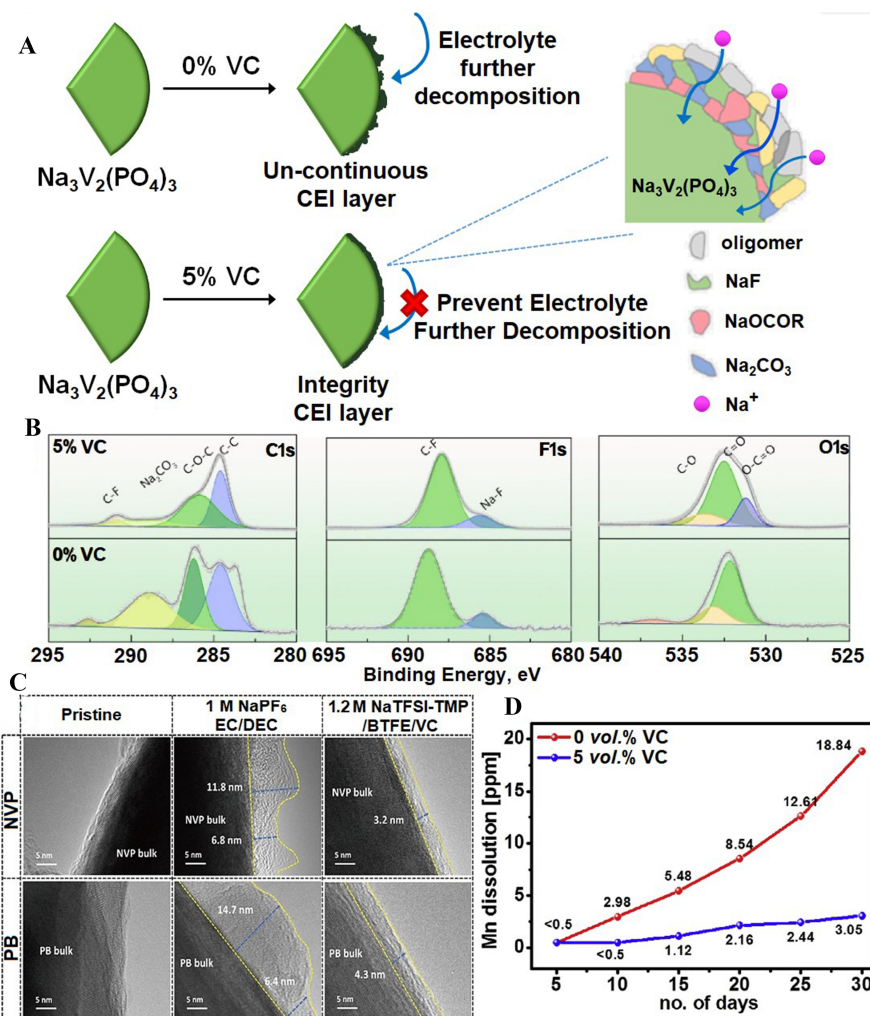


Figure 11. The effect of VC on SIB cathodes. (A) Illustration of the function of VC additives on the surface of $\text{Na}_3\text{V}_2(\text{PO}_4)_3/\text{C}$ cathode; (B) XPS spectra of CEI layer covered on $\text{Na}_3\text{V}_2(\text{PO}_4)_3/\text{C}$ cathode cycled in different electrolytes (0% vol. vs. 5% vol. VC) after the first cycle, Reproduced from ref.^[131], copyright 2021 Elsevier; (C) Ex situ HRTEM images of NVP and PB electrodes cycled in 1M NaPF_6 -EC/DEC and 1.2M $\text{NaTFSI-TMP/BTFE/VC}$ electrolyte, Reproduced from ref.^[132], copyright 2021 Wiley; (D) Amount of manganese dissolution detected by immersing $\text{Na}_2\text{MnSiO}_4$ electrodes in the respective electrolytes (with 0% vol. vs. 5% vol. VC) at room temperature for 30 days, Reproduced from ref.^[133], copyright 2017 Elsevier. BTFE: Bis(trifluoromethanesulfonyl)imide; CEI: cathode electrolyte interphase; DEC: diethyl carbonate; NaTFSI: sodium bis(trifluoromethanesulfonyl)imide; SIB: sodium-ion battery; TMP: trimethyl phosphate; VC: vinylene carbonate; XPS: X-ray photoelectron spectroscopy.

electrolyte additives, PS led to the formation of a CEI enriched with sulfates^[69]. The effects of PS, PES, and DTD on a $\text{Na}(\text{Ni}_{0.4}\text{Mn}_{0.4}\text{Cu}_{0.1}\text{Ti}_{0.1})_{0.999}\text{La}_{0.001}\text{O}_2$ cathode with 1 M NaPF_6 in EC/DMC (1/1) electrolyte were compared in the research of Zhang *et al.*^[59]. Both cells containing the PS and DTD additive showed increased cell capacity retention of 82.0% and 79.4%, respectively, compared with the one of 58.7%. DTD and PS contributed to the formation of a CEI with sulfates and sulfites [Figure 12B], which passivated the cathode surface and prevented electrolyte oxidation. PES, however, consumed a large amount of Na-ions during its decomposition and caused cracking in the $\text{Na}(\text{Ni}_{0.4}\text{Mn}_{0.4}\text{Cu}_{0.1}\text{Ti}_{0.1})_{0.999}\text{La}_{0.001}\text{O}_2$ cathode.

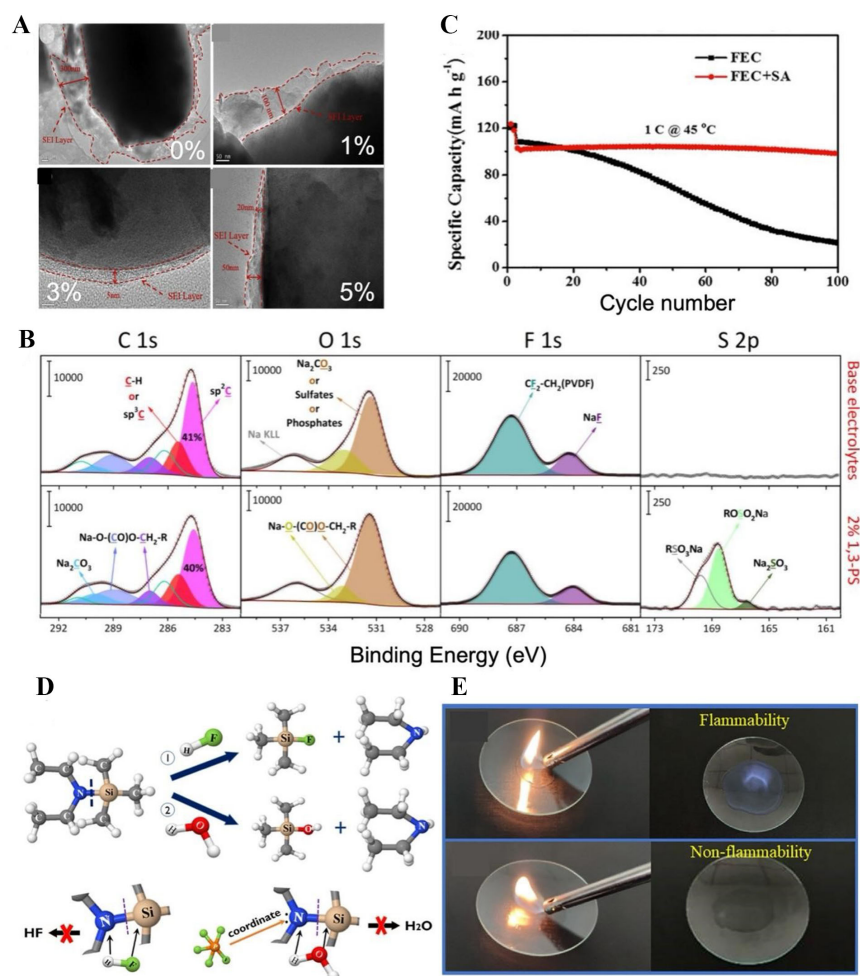


Figure 12. The effect of additives beyond FEC and VC. (A) TEM images of $\text{Na}_{0.76}\text{Ni}_{0.3}\text{Fe}_{0.4}\text{Mn}_{0.3}\text{O}_2$ particles after working in batteries with electrolytes containing various concentrations of ADN (0%, 1%, 3%, 5%). Reproduced from ref^[135], copyright 2018 Elsevier; (B) The high-resolution C 1s, O 1s, F 1s, and S 2p XPS spectra of NMCT-La electrodes cycled in base electrolytes with and without 2% 1,3-PS additive after the first cycle. Reproduced from ref^[59], Copyright 2022 Elsevier; (C) The cyclic performance of Na/NLNC cell cycled at a high temperature of 45 °C. Reproduced from ref^[99], copyright 2021 Wiley; (D) The molecule structure of DETMSA and the reactions with HF and with H_2O by breaking the Si-N bond. Reproduced from ref^[141], copyright 2022 Springer Science + Business Media; (E) Digital photographs of flammability tests for EC-DEC-FEC electrolytes and the concentrated HT12 and HT12-F electrolytes. Reproduced from ref^[142], copyright 2022 Elsevier. DEC: Diethyl carbonate; DETMSA: N, N-diethyltrimethylsilylamine; EC: ethylene carbonate; FEC: fluoroethylene carbonate; SA: succinic anhydride; TEM: transmission electron microscopy; VC: vinylene carbonate; XPS: X-ray photoelectron spectroscopy; 1,3-PS: 1,3-propylene sulfite.

Synergistic additive combinations

By combining the effects of multiple additives, it is possible to create highly efficient and electrochemically performing SIBs. Che *et al.* employed three additives simultaneously, including FEC, DTD, and PST, with $\text{NaNi}_{1/3}\text{Fe}_{1/3}\text{Mn}_{1/3}\text{O}_2$ as the cathode. The cell containing the three additives achieved capacity retention of 92.2% after 1,000 cycles^[70]. The extended lifetime was due to the formation of a dense CEI that prevented the dissolution of TMs. In Fan *et al.*'s research, FEC and SA were utilized in conjunction to create a higher-performance SIB with the $\text{Na}_{0.6}\text{Li}_{0.15}\text{Ni}_{0.15}\text{Mn}_{0.55}\text{Cu}_{0.15}\text{O}_2$ cathode [Figure 12C]^[99]. After 150 cycles, it was shown that a cell with both SA and FEC had capacity retention of 89.9%, while a cell with FEC alone had a retention of 54.6%, which was attributed to a more intact and homogenous CEI layer.

A combination of four additives (NaODFB, PS, VC, SN) were also utilized to improve the performance of SIBs with the $\text{Na}_3\text{V}_2(\text{PO}_4)_2\text{F}_3$ cathode at a high temperature^[69]. The capacity retention of 99% after 60 cycles was achieved at a temperature of 55 °C, and it was discovered that the combination of VC and SN additive is useful in creating a stable CEI layer. Various additive combinations of FEC, VC, PES, DTD, and TTSPi were also assessed using 0.35 M NaBOB in TEP electrolyte with Prussian white material^[138]. Cells containing combinations of PES + DTD as well as PES + TTSPi demonstrated improvements in the initial CE and capacity retention compared to cells without additives due to the formation of benign CEIs.

While the use of multiple electrolyte additives can prove beneficial to battery functionality, certain combinations can have negative effects on cell electrochemical performance. For instance, Nimkar *et al.* noted in their finding^[139] that a mixture of PC and FEC additives performed better than a combination of PC, FEC, and DFEC with the $\text{Na}_{0.44}\text{MnO}_2$ cathode. This was attributed to a thick CEI generated by the double-substitution of FEC and DFEC.

Function on water scavenging

Even short exposures of layered oxide cathodes to moisture can alter their surface chemistry and lead to detrimental effects on battery performance, primarily regarding battery capacity retention and CE. H_2O molecules could occupy the position of Na-ions in cathodes, thus hindering Na^+ cation diffusion^[140], in addition to its side reactions with PF_6^- anion and a generation of HF within the electrolytes. Chen *et al.*^[141] combated this issue using N, N-diethyltrimethylsilylamine (DETMSA) additive within 1 M NaPF_6 in EC:DEC (1:1, by *vol.*) electrolyte in the cells containing the $\text{Na}_x[\text{Ni}_w\text{Mn}_x\text{Mg}_y\text{Ti}_z]\text{O}_2$ cathode. DETMSA acted as a water scavenging additive and contributed to the creation of more robust CEIs [Figure 12D]. The additive significantly improved the cyclability by increasing the capacity retention from 39% to 79% after 500 cycles. Functionally, silicon atoms detached from the DETMSA molecule stabilized the SEI. The multifunctional additive, BSTFA, similar to DETMSA, was used within the ultralow-concentration electrolyte of 0.3 M NaPF_6 in EC:PC (1:1, by *vol.*) in the cells containing a $\text{Na}_3\text{V}_2(\text{PO}_4)_3$ cathode, as described in the report of Jiang *et al.*^[89]. BSTFA was able to suppress the NaPF_6 decomposition by reacting with trace amounts of moisture and removing H_2O and HF from the cell. Additionally, CEI stability was improved via the formation of a NaF-rich, organic species-dominated interphase.

Additives for improving safety

The thermal stability of SIBs often declines significantly when deviating from room temperature, and in extreme cases, fires and complete battery failures can occur^[143]. The electrolytes used in state-of-the-art SIBs are usually composed of a mixture of flammable carbonate-based solvents (e.g., EC, DMC, PC), which are one of the primary safety hazards associated with SIBs. To enhance the inherent safety of SIBs, tremendous efforts have been devoted to suppressing electrolyte flammability. Feng *et al.* tested the performance of tri(2,2,2-trifluoroethyl) phosphite (TFEP), dimethyl methylphosphonate (DMMP), methyl nonafluorobutyl ether (MFE), and TMP as non-flammable co-solvents with Prussian blue cathodes. They found MFE to be the most promising, as it showed an insignificant effect on sodium insertion reactions at electrodes and good compatibility with the cathode^[144]. Similar work of Zeng *et al.*^[145] showed that electrochemical performance of Prussian blue cathodes can be improved in non-flammable fluorinated electrolyte 0.9M $\text{NaPF}_6/\text{FEC-TFEC}$ (3:7 by *vol.*), where TFEC is di-(2,2,2-trifluoroethyl carbonate). As reported by Jin *et al.*^[31], NaFSI/TEP/TTE (1/1.5/2 in mole) electrolyte is non-flammable and highly efficient in SIBs with $\text{NaCu}_{1/9}\text{Ni}_{2/9}\text{Fe}_{1/3}\text{Mn}_{1/3}\text{O}_2$ cathode materials. The SIBs with this electrolyte exhibited excellent cycling stability and capacity retention of 94.8% after 500 cycles. This was, in part, due to the presence of a stable and uniform CEI layer (confirmed by XPS and TEM) with a high inorganic composition and increased amounts of S- and F-based compounds, which suppressed cathode surface reconstruction and electrolyte dissolution.

According to Jia *et al.*^[146], the flammability of an electrolyte is not necessarily the determining factor in superior cell safety. The reactivity between charged electrodes and electrolytes at elevated temperatures often outweighs the flammability of the bulk electrolyte in terms of effects on battery safety. Therefore, the use of suitable electrolyte additives could affect cell safety by modifying the interphase, which has been demonstrated with LIBs^[147,148]. In terms of SIBs, Yu *et al.*^[142] reported that the use of FEC additives in the solvent of 1,1,2,2-tetrafluoroethyl-2,2,3,3-tetrafluoropropyl ether (F-EPE):TMP (1:2 by *vol.*) shows improvements in both safety and capacity retention over a traditional EC:DEC (1:2 by *vol.*) electrolyte [Figure 12E]. This is due to the generation of a dense and robust CEI layer. However, it is difficult to distinguish the effect of the CEI on cell safety due to the non-flammability of F-EPE and TMP. Future studies on the effect of CEI chemistries and structures, tuned by different electrolyte additives, on the thermal stability of SIBs are highly encouraged.

CONCLUSION AND OUTLOOK

Conclusion

Substantial research efforts have been devoted to the wide commercialization of SIBs as complementary energy storage systems of LIBs in several sectors, mainly including transportation (e.g., low-speed EVs, e-scooters, e-bikes) and large-scale stationary energy storage. Achieving an extremely long lifetime is essential to accelerate the widespread adoption of SIBs in these applications. Although limited success has been achieved, much effort is aimed at upgrading the performance of SIBs by developing new materials chemistry to replace those currently in use. The development of electrolyte additives is an equivalently important research direction aimed at improving the performance of SIBs by extending cell lifetime and decreasing safety concerns. This review has summarized various types of electrolyte additives [Figure 13] used in current SIBs. The anode additives introduced here are classified based on their applications in specific electrode materials, while the cathode additives are discussed based on their functions. To summarize this review, Figure 14 clearly divides all additives into SEI-forming, CEI-forming, and additives that contribute to both SEI- and CEI-layers with an optimal amount. Although significant efforts have been devoted to improving the performance of SIBs using electrolyte additives, many challenges still need to be overcome in this area, some of which are discussed below.

Outlook

· **Enhance the tolerance to extreme conditions:** batteries are required to maintain excellent performance at extreme conditions (i.e., fast charging, high and low temperature) due to the operational environment or conditions of applications. Proper modifications of SEI and CEI by using electrolyte additives are the key to regulating interphase impedance, preventing side reactions between electrolytes and electrodes, and improving cell performance under extreme conditions. In addition, the balance of cell lifetime and rate capability at a wide temperature range must be carefully considered in the study of electrolyte additives. Many of the earlier approaches focus only on improving performance at one temperature while compromising the performance of cells at other temperatures. It is important to design electrolyte additives for fast charging and operating within a wide temperature range, long-term cycling, and calendar lifetime.

· **Developing and understanding a mixture of additives:** researchers are likely to focus on understanding the fundamental mechanisms and interactions between additives, electrolytes, and electrode materials. The function of one electrolyte additive on one electrode is relatively simple to understand. However, its beneficial effect may not ameliorate every property of the electrode and could even have a negative impact on another property. With this in mind, the development of electrolyte additive combinations may be a viable solution. For example, prop-1-ene-1,3-sultone, TMSPi, and ethylene sulfate can produce a synergistic effect to inhibit gas evolution, control impedance growth, and extend cell lifetime in carbonate-based electrolytes for LIBs^[147]. Therefore, investigating the interaction discipline between different electrolyte additives for the development of SIB electrolyte additives is of great significance.

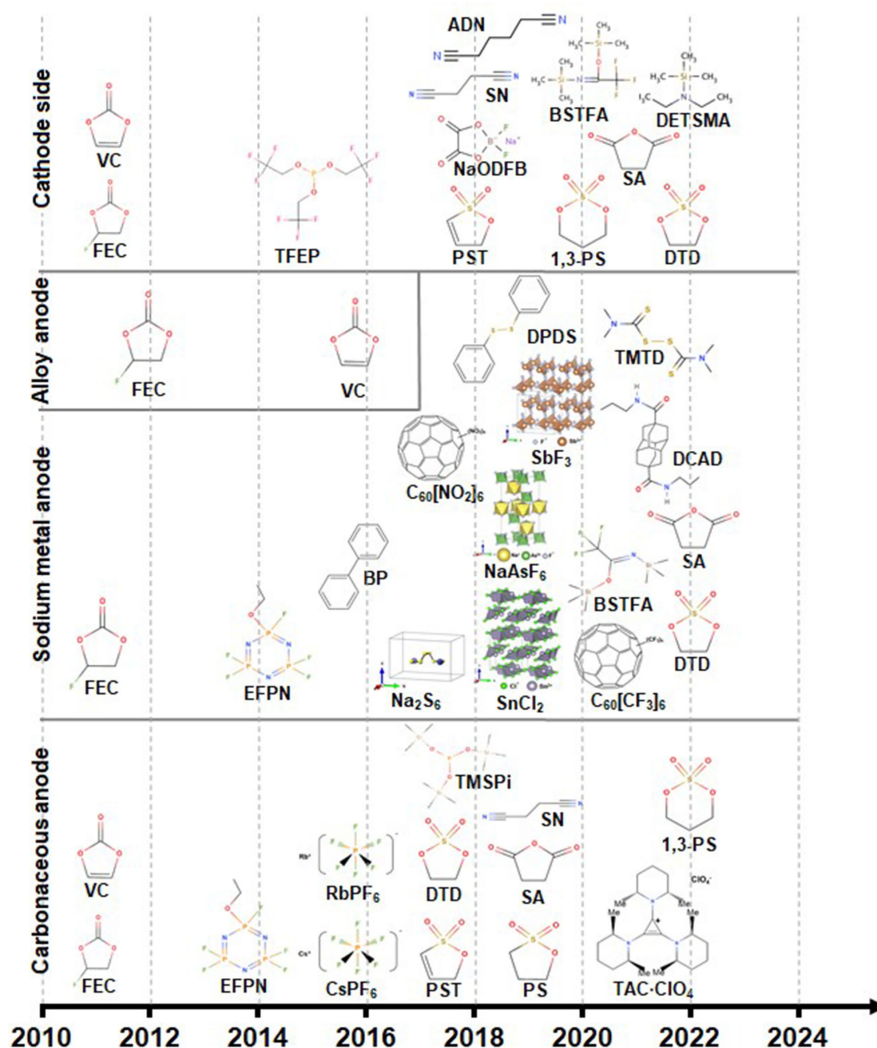


Figure 13. A summarized timeline of the development of selected electrolyte additives for SIBs. BP: Biphenyl; BSTFA: acetamide (N, O-bis(trimethylsilyl) trifluoroacetamide); DCAD: bis-*N,N'*-propyl-4,9-dicarboxamidodiamantane; DPDS: diphenyl disulfide; DTD: 1,3,2-dioxathiolane-2,2-dioxide; EFPN: ethoxy(pentafluoro)cyclotriphosphazene; FEC: fluoroethylene carbonate; NaODFB: sodium (oxalate) difluoro borate; PS: 1,3-propane sultone; PST: prop-1-ene-1,3-sultone; SA: succinic anhydride; SIBs: sodium-ion batteries; SN: succinonitrile; TFEP: tri(2,2,2-trifluoroethyl) phosphite; TMSPI: tris(trimethylsilyl) phosphite; TMTD: tetramethylthiuram disulfide; VC: vinyl carbonate; 1,3-PS: 1,3-propylene sulfite.

· **Understanding the effect of additives on the cathode-anode interaction:** a cathode and an anode are not independent parts within one cell due to their interactions. For example, Xiong *et al.*^[149] suggested that other oxidized species can be produced at the cathode and consumed at the anode as well, leading to a lower rate of impedance growth at the cathode. Electrolyte additives could affect such an interaction process, especially when they are not fully consumed during SEI/CEI formation and evolution. Therefore, it is important to systematically study the effects of additives and additive blends on these electrode/electrode interactions. In our opinion, high-temperature storage experiments on charged cathodes and anodes with isolation are the most efficient methods to identify such an effect for SIBs^[149].

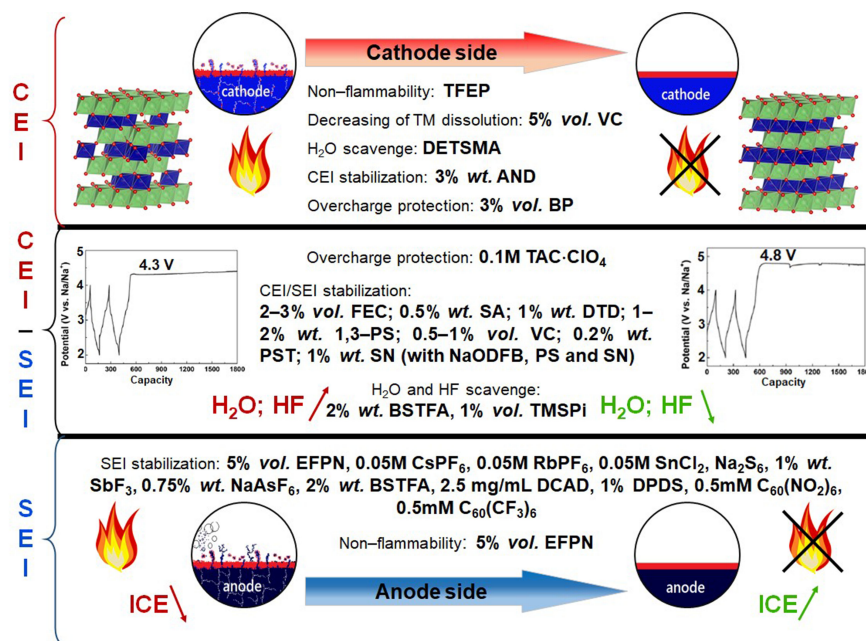


Figure 14. An optimal amount for additives in SIBs electrolyte and its characterization by functional mechanisms and contribution to SEI- or CEI-layer formation. BP: Biphenyl; BSTFA: acetamide (N, O-bis(trimethylsilyl) trifluoroacetamide; CEI: cathode electrolyte interphase; DTD: 1,3,2-dioxathiolane-2,2-dioxide; EFPN: ethoxy(pentafluoro)cyclotriphosphazene; FEC: fluoroethylene carbonate; ICE: initial coulombic efficiency; NaODFB: sodium (oxalate) difluoro borate; PS: 1,3-propane sultone; PST: prop-1-ene-1,3-sultone; SA: succinic anhydride; SEI: solid-state electrolyte interphase; SIBs: sodium-ion batteries; SN: succinonitrile; TFEP: tri(2,2,2-trifluoroethyl) phosphite; VC: vinyl carbonate; 1,3-PS: 1,3-propylene sulfite.

• **Developing additives for improving safety:** safety remains the most important parameter in the development of non-aqueous SIBs. One of the critical factors contributing to battery safety is thermal runaway, which can occur due to reactions between charged electrodes and electrolytes at elevated temperatures. Ma *et al.*^[148] suggested the use of electrolyte additives (e.g., VC) to suppress such reactions and enhance cell safety for LIBs. However, at present, the corresponding research on electrolyte additives is still scanty for SIBs. Hence, a lot of efforts still need to be directed toward additive development for future safer applications.

• **Understanding the characteristics of electrolyte additives:** using a proper amount of electrolyte additives is the key to achieving an optimized cell performance. Either cathode or anode materials may not be fully passivated with inadequate additives, which will result in solvents decomposition and cell lifetime decay. An excess amount of additives could form a thicker SEI/CEI with an increased impedance or could be decomposed into gaseous by-products. Understanding the fate of electrolyte additives and the nature of the by-products of their reactions during formation and cycling is critical to determine the optimized additives amount. According to Petibon *et al.*^[150,151], the use of gas chromatography coupled with mass spectrometry and thermal conductivity detector (GC-MS/TCD) combined with theoretical calculations could reveal the fate of electrolyte additives and understand the way additives work.

DECLARATIONS

Authors' contributions

Analyzed data and prepared sections 1, 3, and 5: Shipitsyn V, Ma L

Analyzed data and prepared sections 2 and 4: AntrAsian N, Soni V, Mu L

Supervised the study and revised the manuscript: Ma L, Mu L

The manuscript was written through the contributions of all authors. All authors have given approval to the final version of the manuscript.

Availability of data and materials

All data that support the findings of this study are presented in the manuscript. Sources of data are provided in this paper.

Financial support and sponsorship

Lin Ma at UNC Charlotte acknowledges the support of the US National Science Foundation under Award (No. 2301719). Dr. Mu is grateful for the start-up funding provided by the School of Engineering for Matter, Transport, and Energy at Arizona State University.

Conflicts of interest

All authors declared that there are no conflicts of interest.

Ethical approval and consent to participate

Not applicable.

Consent for publication

Not applicable.

Copyright

© The Author(s) 2023.

REFERENCES

1. Yabuuchi N, Kubota K, Dahbi M, Komaba S. Research development on sodium-ion batteries. *Chem Rev* 2014;114:11636-82. [DOI](#) [PubMed](#)
2. Vaalma C, Buchholz D, Weil M, Passerini S. A cost and resource analysis of sodium-ion batteries. *Nat Rev Mater* 2018;3:18013. [DOI](#)
3. Delmas C. Sodium and sodium-ion batteries: 50 years of research. *Adv Energy Mater* 2018;8:1703137. [DOI](#)
4. Hwang JY, Myung ST, Sun YK. Sodium-ion batteries: present and future. *Chem Soc Rev* 2017;46:3529-614. [DOI](#) [PubMed](#)
5. Chayambuka K, Mulder G, Danilov DL, Notten PHL. Sodium-ion battery materials and electrochemical properties reviewed. *Adv Energy Mater* 2018;8:1800079. [DOI](#)
6. Fang C, Huang Y, Zhang W, et al. Routes to high energy cathodes of sodium-ion batteries. *Adv Energy Mater* 2016;6:1501727. [DOI](#)
7. Xiao J, Li X, Tang K, et al. Recent progress of emerging cathode materials for sodium ion batteries. *Mater Chem Front* 2021;5:3735-64. [DOI](#)
8. Xiang X, Zhang K, Chen J. Recent advances and prospects of cathode materials for sodium-ion batteries. *Adv Mater* 2015;27:5343-64. [DOI](#)
9. Bommier C, Ji X. Electrolytes, SEI formation, and binders: a review of nonelectrode factors for sodium-ion battery anodes. *Small* 2018;14:e1703576. [DOI](#) [PubMed](#)
10. Song J, Xiao B, Lin Y, Xu K, Li X. Interphases in sodium-ion batteries. *Adv Energy Mater* 2018;8:1703082. [DOI](#)
11. Ponrouch A, Monti D, Boschini A, Steen B, Johansson P, Palacín MR. Non-aqueous electrolytes for sodium-ion batteries. *J Mater Chem A* 2015;3:22-42. [DOI](#)
12. Lao M, Zhang Y, Luo W, Yan Q, Sun W, Dou SX. Alloy-based anode materials toward advanced sodium-ion batteries. *Adv Mater* 2017;29:1700622. [DOI](#) [PubMed](#)
13. Yu P, Tang W, Wu F, et al. Recent progress in plant-derived hard carbon anode materials for sodium-ion batteries: a review. *Rare Met* 2020;39:1019-33. [DOI](#)
14. Chang G, Zhao Y, Dong L, et al. A review of phosphorus and phosphides as anode materials for advanced sodium-ion batteries. *J Mater Chem A* 2020;8:4996-5048. [DOI](#)
15. Goodenough JB. Evolution of strategies for modern rechargeable batteries. *Acc Chem Res* 2013;46:1053-61. [DOI](#) [PubMed](#)
16. Xu K. Electrolytes and interphases in Li-ion batteries and beyond. *Chem Rev* 2014;114:11503-618. [DOI](#) [PubMed](#)
17. Jin Y, Xu Y, Le PML, et al. Highly reversible sodium ion batteries enabled by stable electrolyte-electrode interphases. *ACS Energy*

- Lett* 2020;5:3212-20. DOI
18. Mu L, Feng X, Kou R, et al. Deciphering the cathode-electrolyte interfacial chemistry in sodium layered cathode materials. *Adv Energy Mater* 2018;8:1801975. DOI
 19. Han B, Zou Y, Zhang Z, et al. Probing the Na metal solid electrolyte interphase via cryo-transmission electron microscopy. *Nat Commun* 2021;12:3066. DOI PubMed PMC
 20. Park J, Ku K, Son SB, et al. Effect of electrolytes on the cathode-electrolyte interfacial stability of Fe-based layered cathodes for sodium-ion batteries. *J Electrochem Soc* 2022;169:030536. DOI
 21. Moez I, Susanto D, Chang W, Lim HD, Chung KY. Artificial cathode electrolyte interphase by functional additives toward long-life sodium-ion batteries. *Chem Eng J* 2021;425:130547. DOI
 22. Bodenes L, Darwiche A, Monconduit L, Martinez H. The solid electrolyte interphase a key parameter of the high performance of Sb in sodium-ion batteries: comparative X-ray photoelectron spectroscopy study of Sb/Na-ion and Sb/Li-ion batteries. *J Power Sources* 2015;273:14-24. DOI
 23. Zhang X, Qiao Y, Guo S, et al. Manganese-based Na-rich materials boost anionic redox in high-performance layered cathodes for sodium-ion batteries. *Adv Mater* 2019;31:e1807770. DOI PubMed
 24. Fondard J, Irisarri E, Courrèges C, Palacin MR, Ponrouch A, Dedryvère R. SEI composition on hard carbon in Na-ion batteries after long cycling: influence of salts (NaPF₆, NaTFSI) and additives (FEC, DMCF). *J Electrochem Soc* 2020;167:070526. DOI
 25. Ghigna P, Quartarone E. Operando x-ray absorption spectroscopy on battery materials: a review of recent developments. *J Phys Energy* 2021;3:032006. DOI
 26. Chen M, Chou SL, Dou SX. Understanding challenges of cathode materials for sodium-ion batteries using synchrotron-based X-ray absorption spectroscopy. *Batteries Supercaps* 2019;2:842-51. DOI
 27. Wang PF, Xiao Y, Piao N, et al. Both cationic and anionic redox chemistry in a P2-type sodium layered oxide. *Nano Energy* 2020;69:104474. DOI
 28. Huang J, Guo X, Du X, et al. Nanostructures of solid electrolyte interphases and their consequences for micro-sized Sn anodes in sodium ion batteries. *Energy Environ Sci* 2019;12:1550-7. DOI
 29. Hirsh HS, Sayahpour B, Shen A, et al. Role of electrolyte in stabilizing hard carbon as an anode for rechargeable sodium-ion batteries with long cycle life. *Energy Storage Mater* 2021;42:78-87. DOI
 30. Song H, Su J, Wang C. Multi-ions electrolyte enabled high performance voltage tailorable room-temperature Ca-metal batteries. *Adv Energy Mater* 2021;11:2003685. DOI
 31. Jin Y, Xu Y, Le PML, et al. Highly reversible sodium ion batteries enabled by stable electrolyte-electrode interphases. *ACS Energy Lett* 2020;5:3212-20. DOI
 32. Andre D, Meiler M, Steiner K, Wimmer C, Soczka-Guth T, Sauer DU. Characterization of high-power lithium-ion batteries by electrochemical impedance spectroscopy. I. Experimental investigation. *J Power Sources* 2011;196:5334-41. DOI
 33. Walther F, Koerver R, Fuchs T, et al. Visualization of the interfacial decomposition of composite cathodes in argyrodite-based all-solid-state batteries using time-of-flight secondary-ion mass spectrometry. *Chem Mater* 2019;31:3745-55. DOI
 34. Schwieters T, Evertz M, Mense M, Winter M, Nowak S. Lithium loss in the solid electrolyte interphase: lithium quantification of aged lithium ion battery graphite electrodes by means of laser ablation inductively coupled plasma mass spectrometry and inductively coupled plasma optical emission spectroscopy. *J Power Sources* 2017;356:47-55. DOI
 35. Kim H, Kim H, Ding Z, et al. Recent progress in electrode materials for sodium-ion batteries. *Adv Energy Mater* 2016;6:1600943. DOI
 36. Dou X, Hasa I, Saurel D, et al. Hard carbons for sodium-ion batteries: structure, analysis, sustainability, and electrochemistry. *Mater Today* 2019;23:87-104. DOI
 37. Zhao LF, Hu Z, Lai WH, et al. Hard carbon anodes: fundamental understanding and commercial perspectives for Na-ion batteries beyond Li-ion and K-ion counterparts. *Adv Energy Mater* 2021;11:2002704. DOI
 38. Komaba S, Murata W, Ishikawa T, et al. Electrochemical Na insertion and solid electrolyte interphase for hard-carbon electrodes and application to Na-ion batteries. *Adv Funct Mater* 2011;21:3859-67. DOI
 39. Komaba S, Ishikawa T, Yabuuchi N, Murata W, Ito A, Ohsawa Y. Fluorinated ethylene carbonate as electrolyte additive for rechargeable Na batteries. *ACS Appl Mater Interfaces* 2011;3:4165-8. DOI PubMed
 40. Dahbi M, Nakano T, Yabuuchi N, et al. Effect of hexafluorophosphate and fluoroethylene carbonate on electrochemical performance and the surface layer of hard carbon for sodium-ion batteries. *ChemElectroChem* 2016;3:1856-67. DOI
 41. Tang K, Fu L, White RJ, et al. Hollow carbon nanospheres with superior rate capability for sodium-ion based batteries. *Adv Energy Mater* 2012;2:873-7. DOI
 42. Luo W, Schardt J, Bommier C, et al. Carbon nanofibers derived from cellulose nanofibers as a long-life anode material for rechargeable sodium-ion batteries. *J Mater Chem A* 2013;1:10662-6. DOI
 43. Zhou X, Guo Y. Highly disordered carbon as a superior anode material for room-temperature sodium-ion batteries. *ChemElectroChem* 2014;1:83-6. DOI
 44. Xie H, Wu Z, Wang Z, et al. Solid electrolyte interface stabilization via surface oxygen species functionalization in hard carbon for superior performance sodium-ion batteries. *J Mater Chem A* 2020;8:3606-12. DOI
 45. Bommier C, Luo W, Gao WY, Greaney A, Ma S, Ji X. Predicting capacity of hard carbon anodes in sodium-ion batteries using porosity measurements. *Carbon* 2014;76:165-74. DOI

46. Ponrouch A, Goñi AR, Palacín MR. High capacity hard carbon anodes for sodium ion batteries in additive free electrolyte. *Electrochem Commun* 2013;27:85-8. DOI
47. Zhu YE, Gu H, Chen YN, Yang D, Wei J, Zhou Z. Hard carbon derived from corn straw piths as anode materials for sodium ion batteries. *Ionics* 2018;24:1075-81. DOI
48. Jin J, Yu BJ, Shi ZQ, Wang CY, Chong CB. Lignin-based electrospun carbon nanofibrous webs as free-standing and binder-free electrodes for sodium ion batteries. *J Power Sources* 2014;272:800-7. DOI
49. Yang T, Qian T, Wang M, et al. A sustainable route from biomass byproduct okara to high content nitrogen-doped carbon sheets for efficient sodium ion batteries. *Adv Mater* 2016;28:539-45. DOI
50. Cao Y, Xiao L, Sushko ML, et al. Sodium ion insertion in hollow carbon nanowires for battery applications. *Nano Lett* 2012;12:3783-7. DOI
51. Lotfabad EM, Ding J, Cui K, et al. High-density sodium and lithium ion battery anodes from banana peels. *ACS Nano* 2014;8:7115-29. DOI
52. Jiang X, Liu X, Zeng Z, et al. A bifunctional fluorophosphate electrolyte for safer sodium-ion batteries. *iScience* 2018;10:114-22. DOI PubMed PMC
53. Li Y, Xu S, Wu X, et al. Amorphous monodispersed hard carbon micro-spherules derived from biomass as a high performance negative electrode material for sodium-ion batteries. *J Mater Chem A* 2015;3:71-7. DOI
54. Li W, Zeng L, Yang Z, et al. Free-standing and binder-free sodium-ion electrodes with ultralong cycle life and high rate performance based on porous carbon nanofibers. *Nanoscale* 2014;6:693-8. DOI
55. Ding J, Wang H, Li Z, et al. Carbon nanosheet frameworks derived from peat moss as high performance sodium ion battery anodes. *ACS Nano* 2013;7:11004-15. DOI
56. Liu X, Jiang X, Zeng Z, et al. High capacity and cycle-stable hard carbon anode for nonflammable sodium-ion batteries. *ACS Appl Mater Interfaces* 2018;10:38141-50. DOI
57. Li Y, Hu YS, Titirici MM, Chen L, Huang X. Hard carbon microtubes made from renewable cotton as high-performance anode material for sodium-ion batteries. *Adv Energy Mater* 2016;6:1600659. DOI
58. Li Y, Lu Y, Meng Q, et al. Regulating pore structure of hierarchical porous waste cork-derived hard carbon anode for enhanced Na storage performance. *Adv Energy Mater* 2019;9:1902852. DOI
59. Zhang Q, Wang Z, Li X, et al. Comparative study of 1,3-propane sultone, prop-1-ene-1,3-sultone and ethylene sulfate as film-forming additives for sodium ion batteries. *J Power Sources* 2022;541:231726. DOI
60. Shao Y, Xiao J, Wang W, et al. Surface-driven sodium ion energy storage in nanocellular carbon foams. *Nano Lett* 2013;13:3909-14. DOI
61. Feng J, An Y, Ci L, Xiong S. Nonflammable electrolyte for safer non-aqueous sodium batteries. *J Mater Chem A* 2015;3:14539-44. DOI
62. Luo W, Bommier C, Jian Z, et al. Low-surface-area hard carbon anode for Na-ion batteries via graphene oxide as a dehydration agent. *ACS Appl Mater Interfaces* 2015;7:2626-31. DOI
63. Kim DH, Kang B, Lee H. Comparative study of fluoroethylene carbonate and succinic anhydride as electrolyte additive for hard carbon anodes of Na-ion batteries. *J Power Sources* 2019;423:137-43. DOI
64. Bai P, Han X, He Y, et al. Solid electrolyte interphase manipulation towards highly stable hard carbon anodes for sodium ion batteries. *Energy Stor Mater* 2020;25:324-33. DOI
65. Che H, Liu J, Wang H, et al. Rubidium and cesium ions as electrolyte additive for improving performance of hard carbon anode in sodium-ion battery. *Electrochem Commun* 2017;83:20-3. DOI
66. Wang J, Yamada Y, Sodeyama K, et al. Fire-extinguishing organic electrolytes for safe batteries. *Nat Energy* 2018;3:22-9. DOI
67. Zhang J, Wang DW, Lv W, et al. Achieving superb sodium storage performance on carbon anodes through an ether-derived solid electrolyte interphase. *Energy Environ Sci* 2017;10:370-6. DOI
68. Cometto C, Yan G, Mariyappan S, Tarascon JM. Means of using cyclic voltammetry to rapidly design a stable DMC-based electrolyte for Na-ion batteries. *J Electrochem Soc* 2019;166:A3723-30. DOI
69. Yan G, Reeves K, Foix D, et al. A new electrolyte formulation for securing high temperature cycling and storage performances of Na-ion batteries. *Adv Energy Mater* 2019;9:1901431. DOI
70. Che H, Yang X, Wang H, et al. Long cycle life of sodium-ion pouch cell achieved by using multiple electrolyte additives. *J Power Sources* 2018;407:173-9. DOI
71. Dugas R, Ponrouch A, Gachot G, David R, Palacín MR, Tarascon JM. Na reactivity toward carbonate-based electrolytes: the effect of FEC as additive. *J Electrochem Soc* 2016;163:A2333-9. DOI
72. Liu Q, Mu D, Wu B, Wang L, Gai L, Wu F. Density functional theory research into the reduction mechanism for the solvent/additive in a sodium-ion battery. *ChemSusChem* 2017;10:786-96. DOI
73. Wang E, Niu Y, Yin YX, Guo YG. Manipulating electrode/electrolyte interphases of sodium-ion batteries: strategies and perspectives. *ACS Materials Lett* 2021;3:18-41. DOI
74. Hu S, Zhao H, Qian Y, et al. Improved high-temperature performance of $\text{LiNi}_{0.5}\text{Co}_{0.2}\text{Mn}_{0.3}\text{O}_2$ /artificial graphite lithium ion pouch cells by difluoroethylene carbonate. *J Energy Storage* 2023;57:106266. DOI
75. Ma L, Glazier SL, Petibon R, et al. A guide to ethylene carbonate-free electrolyte making for Li-ion cells. *J Electrochem Soc* 2017;164:A5008-18. DOI

76. Yu Z, Yu W, Chen Y, et al. Tuning fluorination of linear carbonate for lithium-ion batteries. *J Electrochem Soc* 2022;169:040555. DOI
77. Lee H, Choi S, Choi S, et al. SEI layer-forming additives for $\text{LiNi}_{0.5}\text{Mn}_{1.5}\text{O}_4$ /graphite 5V Li-ion batteries. *Electrochem Commun* 2007;9:801-6. DOI
78. Leggesse EG, Jiang JC. Theoretical study of the reductive decomposition of 1,3-propane sultone: SEI forming additive in lithium-ion batteries. *RSC Adv* 2012;2:5439-46. DOI
79. Liu Q, Xu R, Mu D, et al. Progress in electrolyte and interface of hard carbon and graphite anode for sodium-ion battery. *Carbon Energy* 2022;4:458-79. DOI
80. Xia L, Xia Y, Liu Z. A novel fluorocyclophosphazene as bifunctional additive for safer lithium-ion batteries. *J Power Sources* 2015;278:190-6. DOI
81. Ji W, Huang H, Zhang X, et al. A redox-active organic salt for safer Na-ion batteries. *Nano Energy* 2020;72:104705. DOI PubMed PMC
82. Zheng X, Fu H, Hu C, et al. Toward a stable sodium metal anode in carbonate electrolyte: a compact, inorganic alloy interface. *J Phys Chem Lett* 2019;10:707-14. DOI
83. Wang H, Wang C, Matios E, Li W. Facile stabilization of the sodium metal anode with additives: unexpected key role of sodium polysulfide and adverse effect of sodium nitrate. *Angew Chem* 2018;130:7860-3. DOI
84. Fang W, Jiang H, Zheng Y, et al. A bilayer interface formed in high concentration electrolyte with SbF_3 additive for long-cycle and high-rate sodium metal battery. *J Power Sources* 2020;455:227956. DOI
85. Wang S, Cai W, Sun Z, et al. Stable cycling of Na metal anodes in a carbonate electrolyte. *Chem Commun* 2019;55:14375-8. DOI
86. Jiang Z, Zeng Z, Yang C, et al. Nitrofullerene, a C_{60} -based bifunctional additive with smoothing and protecting effects for stable lithium metal anode. *Nano Lett* 2019;19:8780-6. DOI PubMed
87. Li P, Jiang Z, Huang X, Lu X, Xie J, Cheng S. Nitrofullerene as an electrolyte-compatible additive for high-performance sodium metal batteries. *Nano Energy* 2021;89:106396. DOI
88. Li P, Huang X, Jiang Z, et al. High-rate sodium metal batteries enabled by trifluoromethylfullerene additive. *Nano Res* 2022;15:7172-9. DOI
89. Jiang R, Hong L, Liu Y, et al. An acetamide additive stabilizing ultra-low concentration electrolyte for long-cycling and high-rate sodium metal battery. *Energy Stor Mater* 2021;42:370-9. DOI
90. Kreissl JJA, Langsdorf D, Tkachenko BA, Schreiner PR, Janek J, Schröder D. Incorporating diamondoids as electrolyte additive in the sodium metal anode to mitigate dendrite growth. *ChemSusChem* 2020;13:2661-70. DOI PubMed PMC
91. Zhu M, Wang G, Liu X, et al. Dendrite-free sodium metal anodes enabled by a sodium benzenedithiolate-rich protection layer. *Angew Chem* 2020;132:6658-62. DOI
92. Zhu M, Zhang Y, Yu F, et al. Stable sodium metal anode enabled by an interface protection layer rich in organic sulfide salt. *Nano Lett* 2021;21:619-27. DOI
93. Zhu M, Li L, Zhang Y, et al. An in-situ formed stable interface layer for high-performance sodium metal anode in a non-flammable electrolyte. *Energy Storage Materials* 2021;42:145-53. DOI
94. Rodriguez R, Loeffler KE, Nathan SS, et al. In situ optical imaging of sodium electrodeposition: effects of fluoroethylene carbonate. *ACS Energy Lett* 2017;2:2051-7. DOI
95. Shiraz MHA, Zhao P, Liu J. High-performance sodium-selenium batteries enabled by microporous carbon/selenium cathode and fluoroethylene carbonate electrolyte additive. *J Power Sources* 2020;453:227855. DOI
96. Han M, Zhu C, Ma T, Pan Z, Tao Z, Chen J. In situ atomic force microscopy study of nano-micro sodium deposition in ester-based electrolytes. *Chem Commun* 2018;54:2381-4. DOI PubMed
97. Wang Q, Zhao C, Lv X, et al. Stabilizing a sodium-metal battery with the synergy effects of a sodiophilic matrix and fluorine-rich interface. *J Mater Chem A* 2019;7:24857-67. DOI
98. Pan K, Lu H, Zhong F, Ai X, Yang H, Cao Y. Understanding the electrochemical compatibility and reaction mechanism on Na metal and hard carbon anodes of PC-based electrolytes for sodium-ion batteries. *ACS Appl Mater Interfaces* 2018;10:39651-60. DOI PubMed
99. Fan JJ, Dai P, Shi CG, et al. Synergistic dual-additive electrolyte for interphase modification to boost cyclability of layered cathode for sodium ion batteries. *Adv Funct Mater* 2021;31:2010500. DOI
100. Feng J, Ci L, Xiong S. Biphenyl as overcharge protection additive for nonaqueous sodium batteries. *RSC Adv* 2015;5:96649-52. DOI
101. Baggetto L, Marszewski M, Górka J, Jaroniec M, Veith GM. AISB thin films as negative electrodes for Li-ion and Na-ion batteries. *J Power Sources* 2013;243:699-705. DOI
102. Baggetto L, Keum JK, Browning JF, Veith GM. Germanium as negative electrode material for sodium-ion batteries. *Electrochem Commun* 2013;34:41-4. DOI
103. Baggetto L, Allcorn E, Unocic RR, Manthiram A, Veith GM. Mo_3Sb_7 as a very fast anode material for lithium-ion and sodium-ion batteries. *J Mater Chem A* 2013;1:11163-9. DOI
104. Darwiche A, Marino C, Sougrati MT, Fraisse B, Stievano L, Monconduit L. Better cycling performances of bulk Sb in Na-ion batteries compared to Li-ion systems: an unexpected electrochemical mechanism. *J Am Chem Soc* 2012;134:20805-11. DOI PubMed
105. Ma W, Yin K, Gao H, Niu J, Peng Z, Zhang Z. Alloying boosting superior sodium storage performance in nanoporous tin-antimony

- alloy anode for sodium ion batteries. *Nano Energy* 2018;54:349-59. DOI
106. Kim IT, Kim SO, Manthiram A. Effect of TiC addition on SnSb-C composite anodes for sodium-ion batteries. *J Power Sources* 2014;269:848-54. DOI
107. Kim IT, Allcorn E, Manthiram A. High-performance FeSb-TiC-C nanocomposite anodes for sodium-ion batteries. *Phys Chem Chem Phys* 2014;16:12884-9. DOI PubMed
108. Kim IT, Allcorn E, Manthiram A. Cu₆Sn₅-TiC-C nanocomposite anodes for high-performance sodium-ion batteries. *J Power Sources* 2015;281:11-7. DOI
109. Sadan MK, Choi SH, Kim HH, et al. Effect of sodium salts on the cycling performance of tin anode in sodium ion batteries. *Ionics* 2018;24:753-61. DOI
110. Qian J, Chen Y, Wu L, Cao Y, Ai X, Yang H. High capacity Na-storage and superior cyclability of nanocomposite Sb/C anode for Na-ion batteries. *Chem Commun* 2012;48:7070-2. DOI
111. Ji L, Gu M, Shao Y, et al. Controlling SEI formation on SnSb-porous carbon nanofibers for improved Na ion storage. *Adv Mater* 2014;26:2901-8. DOI
112. Zhang J, Zhang K, Yang J, et al. Engineering solid electrolyte interphase on red phosphorus for long-term and high-capacity sodium storage. *Chem Mater* 2020;32:448-58. DOI
113. Yabuuchi N, Matsuura Y, Ishikawa T, et al. Phosphorus electrodes in sodium cells: small volume expansion by sodiation and the surface-stabilization mechanism in aprotic solvent. *ChemElectroChem* 2014;1:580-9. DOI
114. Dahbi M, Yabuuchi N, Fukunishi M, et al. Black phosphorus as a high-capacity, high-capability negative electrode for sodium-ion batteries: investigation of the electrode/electrolyte interface. *Chem Mater* 2016;28:1625-35. DOI
115. Li M, Muralidharan N, Moyer K, Pint CL. Solvent mediated hybrid 2D materials: black phosphorus - graphene heterostructured building blocks assembled for sodium ion batteries. *Nanoscale* 2018;10:10443-9. DOI PubMed
116. Song J, Wu M, Fang K, Tian T, Wang R, Tang H. NaF-rich interphase and high initial coulombic efficiency of red phosphorus anode for sodium-ion batteries by chemical presodiation. *J Colloid Interface Sci* 2023;630:443-52. DOI
117. Capone I, Hurlbutt K, Naylor AJ, Xiao AW, Pasta M. Effect of the particle-size distribution on the electrochemical performance of a red phosphorus-carbon composite anode for sodium-ion batteries. *Energy Fuels* 2019;33:4651-8. DOI PubMed PMC
118. Jian Z, Zhao B, Liu P, et al. Fe₂O₃ nanocrystals anchored onto graphene nanosheets as the anode material for low-cost sodium-ion batteries. *Chem Commun* 2014;50:1215-7. DOI PubMed
119. Hu Z, Wang L, Zhang K, et al. MoS₂ nanoflowers with expanded interlayers as high-performance anodes for sodium-ion batteries. *Angew Chem Int Ed Engl* 2014;53:12794-8. DOI PubMed
120. Xiong H, Slater MD, Balasubramanian M, Johnson CS, Rajh T. Amorphous TiO₂ nanotube anode for rechargeable sodium ion batteries. *J Phys Chem Lett* 2011;2:2560-5. DOI
121. Dynarowska M, Kotwiński J, Leszczynska M, Marzantowicz M, Krok F. Ionic conductivity and structural properties of Na₂Ti₃O₇ anode material. *Solid State Ionics* 2017;301:35-42. DOI
122. Zhao L, Zhao J, Hu YS, et al. Disodium Terephthalate (Na₂C₈H₄O₄) as high performance anode material for low-cost room-temperature sodium-ion battery. *Adv Energy Mater* 2012;2:962-5. DOI
123. Armand M, Endres F, MacFarlane DR, Ohno H, Scrosati B. Ionic-liquid materials for the electrochemical challenges of the future. *Nat Mater* 2009;8:621-9. DOI PubMed
124. López-herraiz M, Castillo-martínez E, Carretero-gonzález J, Carrasco J, Rojo T, Armand M. Oligomeric-schiff bases as negative electrodes for sodium ion batteries: unveiling the nature of their active redox centers. *Energy Environ Sci* 2015;8:3233-41. DOI
125. Castillo-Martínez E, Carretero-González J, Armand M. Polymeric schiff bases as low-voltage redox centers for sodium-ion batteries. *Angew Chem Int Ed Engl* 2014;53:5341-5. DOI PubMed
126. Huang Y, Zhao L, Li L, Xie M, Wu F, Chen R. Electrolytes and electrolyte/electrode interfaces in sodium-ion batteries: from scientific research to practical application. *Adv Mater* 2019;31:e1808393. DOI PubMed
127. Kucinskis G, Nesterova I, Sarakovskis A, Bikse L, Hodakovska J, Bajars G. Electrochemical performance of Na₂FeP₂O₇/C cathode for sodium-ion batteries in electrolyte with fluoroethylene carbonate additive. *J Alloys Compd* 2022;895:162656. DOI
128. Lee Y, Lee J, Kim H, Kang K, Choi NS. Highly stable linear carbonate-containing electrolytes with fluoroethylene carbonate for high-performance cathodes in sodium-ion batteries. *J Power Sources* 2016;320:49-58. DOI
129. Cheng Z, Mao Y, Dong Q, et al. Fluoroethylene carbonate as an additive for sodium-ion batteries: effect on the sodium cathode. *Acta Phys-Chim Sin* 2019;35:868-75. DOI
130. Wu S, Su B, Kun N, et al. Fluorinated carbonate electrolyte with superior oxidative stability enables long-term cycle stability of Na_{2/3}Ni_{1/3}Mn_{2/3}O₂ cathodes in sodium-ion batteries. *Adv Energy Mater* 2020;11:2002737. DOI
131. Shi J, Ding L, Wan Y, et al. Achieving long-cycling sodium-ion full cells in ether-based electrolyte with vinylene carbonate additive. *J Energy Chem* 2021;57:650-5. DOI
132. Yang Z, He J, Lai WH, et al. Fire-retardant, stable-cycling and high-safety sodium ion battery. *Angew Chem* 2021;133:27292-300. DOI
133. Law M, Ramar V, Balaya P. Na₂MnSiO₄ as an attractive high capacity cathode material for sodium-ion battery. *J Power Sources* 2017;359:277-84. DOI
134. Farhat D, Maibach J, Eriksson H, Edström K, Lemordant D, Ghamouss F. Towards high-voltage Li-ion batteries: reversible cycling of graphite anodes and Li-ion batteries in adiponitrile-based electrolytes. *Electrochimica Acta* 2018;281:299-311. DOI

135. Song X, Meng T, Deng Y, et al. The effects of the functional electrolyte additive on the cathode material $\text{Na}_{0.76}\text{Ni}_{0.3}\text{Fe}_{0.4}\text{Mn}_{0.3}\text{O}_2$ for sodium-ion batteries. *Electrochimica Acta* 2018;281:370-7. DOI
136. Tong B, Song Z, Wan H, et al. Sulfur-containing compounds as electrolyte additives for lithium-ion batteries. *InfoMat* 2021;3:1364-92. DOI
137. Xie D, Zhang M, Wu Y, Xiang L, Tang Y. A flexible dual-ion battery based on sodium-ion quasi-solid-state electrolyte with long cycling life. *Adv Funct Mater* 2020;30:1906770. DOI
138. Welch J, Mogensen R, van Ekeren W, Eriksson H, Naylor AJ, Younesi R. Optimization of sodium bis(oxalato)borate (NaBOB) in triethyl phosphate (TEP) by electrolyte additives. *J Electrochem Soc* 2022;169:120523. DOI
139. Nimkar A, Shpigel N, Malchik F, et al. Unraveling the role of fluorinated alkyl carbonate additives in improving cathode performance in sodium-ion batteries. *ACS Appl Mater Interfaces* 2021;13:46478-87. DOI
140. Zuo W, Qiu J, Liu X, et al. The stability of P2-layered sodium transition metal oxides in ambient atmospheres. *Nat Commun* 2020;11:3544. DOI PubMed PMC
141. Chen L, Kishore B, Song T, Walker M, Dancer C, Kendrick E. Improved lifetime of Na-ion batteries with a water-scavenging electrolyte additive. *Front Energy Res* 2022;10:925430. DOI
142. Yu Y, Che H, Yang X, Deng Y, Li L, Ma ZF. Non-flammable organic electrolyte for sodium-ion batteries. *Electrochem Commun* 2020;110:106635. DOI
143. Hueso KB, Armand M, Rojo T. High temperature sodium batteries: status, challenges and future trends. *Energy Environ Sci* 2013;6:734-49. DOI
144. Feng J, Zhang Z, Li L, Yang J, Xiong S, Qian Y. Ether-based nonflammable electrolyte for room temperature sodium battery. *J Power Sources* 2015;284:222-6. DOI
145. Zeng G, Liu Y, Gu C, et al. A nonflammable fluorinated carbonate electrolyte for sodium-ion batteries. *Acta Phys-Chim Sin* 2020;36:1905006-0. DOI
146. Jia H, Yang Z, Xu Y, et al. Is nonflammability of electrolyte overrated in the overall safety performance of lithium ion batteries? *Advanced Energy Materials* 2023;13:2203144. DOI
147. Ma L, Xia J, Dahn JR. Ternary electrolyte additive mixtures for Li-ion cells that promote long lifetime and less reactivity with charged electrodes at elevated temperatures. *J Electrochem Soc* 2015;162:A1170-4. DOI
148. Ma L, Xia J, Xia X, Dahn JR. The impact of vinylene carbonate, fluoroethylene carbonate and vinyl ethylene carbonate electrolyte additives on electrode/electrolyte reactivity studied using accelerating rate calorimetry. *J Electrochem Soc* 2014;161:A1495-8. DOI
149. Xiong DJ, Petibon R, Nie M, Ma L, Xia J, Dahn JR. Interactions between positive and negative electrodes in Li-ion cells operated at high temperature and high voltage. *J Electrochem Soc* 2016;163:A546-51. DOI
150. Petibon R, Rotermund L, Nelson KJ, Gozdz AS, Xia J, Dahn JR. Study of electrolyte components in Li ion cells using liquid-liquid extraction and gas chromatography coupled with mass spectrometry. *J Electrochem Soc* 2014;161:A1167-72. DOI
151. Petibon R, Chevrier VL, Aiken CP, et al. Studies of the capacity fade mechanisms of LiCoO_2/Si -alloy: graphite cells. *J Electrochem Soc* 2016;163:A1146-56. DOI